LATE HOLOCENE DRY PERIODS RECORDED IN SPELEOTHEMS FROM THE MAYA LOWLANDS OF THE YUCATAN PENINSULA, MEXICO

A THESIS SUBMITTED TO THE FACULTY OF THE GRADUATE SCHOOL
OF THE UNIVERSITY OF MINNESOTA
BY

Erin Alison Endsley

IN PARTIAL FULFILLMENT OF THE REQUIREMENTS
FOR THE DEGREE OF
MASTER OF SCIENCE

May 2007

ACKNOWLEDGEMENTS

There are many people I would like to thank who have assisted or supported me during my career at UMD and while working on completing my thesis. I would like to thank my advisor Christina Gallup for providing me the opportunity to work on this project and for her assistance over the past two years. Thanks to my committee members, Paul Siders and Steve Colman, for their willingness to serve on my committe and provide valuable feedback; Dave Hodell, Mark Brenner, Jason Curtis, and Cara Gentry at the University of Florida for assistance in the field and during stable isotope work at UF; the Minnesota Isotope Lab for their assistance in running samples on the ICP-MS; the faculty and staff of the Department of Geological Science and the Large Lakes Observatory at UMD; fellow graduate students at UMD; and my friends and family, especially my grandparents, who have always been there to support me.

ABSTRACT

Evidence for Holocene droughts in Mesoamerica exists from numerous paleolimnological studies. Speleothems from the Yucatan Peninsula can be used to help constrain the timing, intensity, and regional extent of these droughts. Late Holocene wet/dry cycles are inferred from the oxygen isotope record of speleothem calcite and the timing is constrained using U/Th dating. In the lowland neotropics, there is a strong negative correlation between $\delta^{18}O$ of precipitation and rainfall amount, i.e. the "amount effect". The $\delta^{18}O$ of speleothem calcite can then be used as a proxy for the relative amount of past precipitation in the Maya Lowlands. A speleothem from Cueva Tzabnah, near Tecoh, Yucatan, Mexico, has a basal date of 1240 ±61 yr BP and a top date of 28 ±21 yr BP, indicating growth during most of the Terminal Classic period of Maya prehistory. Oxygen isotopes were measured at 0.5 mm intervals, with an average value of -5.25‰. $\delta^{18}O$ values increase near the hiatuses in speleothem growth, interpreted as evidence for the presence of drought conditions. The relative increases in $\delta^{18}O$ are dated using U/Th methods to constrain the timing of the drought events. In the top 3mm, the mean $\delta^{18}O$ value is 2.49‰ greater than the mean speleothem $\delta^{18}O$ value, and possibly represents drier conditions beginning in the mid-15th century AD consistent with a nearby lake sediment core record from Aguada X'caamal (Hodell et al., 2005). Another speleothem from Cueva Columnas, near Tzucacab, Mexico, has a basal date of 1347 ±63 yr BP and a top date of 520 ±99 yr BP, and a mean $\delta^{18}O$ value of –3.80‰. Both speleothems contain evidence for past climate fluctuations during the Terminal Classic period, including a relatively drier period from about 850-900 AD recorded in both speleothems.

TABLE OF CONTENTS

List of Figures:

List of Tables:

INTRODUCTION

The Maya civilization occupied the Yucatan Peninsula (Figure 1) of Mexico, Guatemala, and Belize since 2000 BC, culminating in a cultural peak during the Classic period (ca 250-900 AD). The Classic Maya civilization experienced a dramatic decline during the late Terminal Classic Period (ca 800-1000 AD), when many large population centers were abandoned and monuments ceased to be built (Sharer, 1994). One of the prominent hypotheses is that a prolonged drought contributed to the demise of the Maya during the late terminal Classic Period. The hypothesis is controversial because accurately dated paleoclimate records from the Maya Lowlands of the Yucatan Peninsula that span the late Holocene (last 2 to 3 thousand years) are needed in order to assess the role climate may have played in the collapse of the Classic Maya civilization. Although paleoclimate studies from lakes indicate drought conditions existed during the late Holocene, these records are not well-constrained. Paleoclimate data from speleothems, which have a much higher resolution and can be accurately dated using U/Th techniques, have the potential to resolve this problem.

The Maya Lowlands of the Yucatan Peninsula consist of a karst landscape that contains numerous caves with abundant speleothems. The growth rates of the speleothems often allow for resolution of climate signals on a sub-decadal timescale. The growth layers can be successfully analyzed for both carbon and oxygen isotopes, which yield valuable data about past climate (White, 2004). Carbon isotopes are useful for recording vegetation changes, possibly resulting from either climate change or human land use, and oxygen isotopes provide information about amount of past precipitation (Harmon et al., 2004).

Despite abundant caves with speleothems, there are relatively few paleoclimatology studies using climate archives from caves from the Yucatan or from central America, especially from the late Holocene. Webster et al., in press, present paleoclimate data from a 3300-yr old stalagmite from Belize. The stalagmite, dated using a combination of U/Th, radiocarbon, and ^{210}Pb methods, reveals evidence for droughts in the Maya Lowlands, including a severe drought lasting from 700-1135 AD, encompassing the terminal Classic Period. Two other studies have also used U/Th techniques to date speleothems from the lowland Neotropics. Lachniet et al. (2004a) documented an early Holocene dry period in Costa Rica, and Lachniet et al. (2004b) studied El Nino/Southern Oscillation and precipitation history over the last 1500 years recorded in calcite from a Panamanian speleothem. Although these studies reveal the ability to use speleothem calcite to obtain a datable climate archive in the Neotropics, speleothems from the northern Yucatan have yet to be dated accurately and precisely using U/Th dating techniques. This is significant, because archeological studies indicate abandonment of Maya settlements in the northern Yucatan occurred between 861-910 AD, whereas abandonment of sites in the western and southeastern lowlands occurred earlier, between 760-810 AD (Gill, 2000). Paleoclimate evidence from speleothems in the northern Yucatan could provide support for the spatial extent and regional timing of droughts in the Maya Lowlands, which can then be correlated with the archeological record.

In this study, U/Th dating methods are used to constrain the climatic changes during the late Holocene as recorded in oxygen isotopes in the "Tecoh" speleothem from Cueva Tzabnah, near Tecoh, Yucatan, and in the "Hobo 5" speleothem from Cueva Columnas, Rancho Hobonil, near Tzucacab, Yucatan.

BACKGROUND

Study Area: Climate and Geology

The Maya Lowlands of the Yucatan Peninsula include the Peten, or central lowlands of Guatemala and Belize, and the Yucatecan, or northern lowlands of the Yucatan Peninsula in Mexico (Morley and Brainerd, 1983). The Yucatan is known as the site of the earliest centers of the Classic Maya civilization, which spread throughout the region and culminated in a cultural peak from the third through the ninth centuries AD (Morley and Brainerd, 1983). Tikal, a population center located in the Peten, may have supported up to 49,000 individuals during the late Classic Period (Haviland, 1969), and population estimates for the Maya Lowlands are as high as 13 million at the peak of the Classic period (Sharer, 1994).

The current climate of the Maya Lowlands is warm, with an average temperature of 25°C. A sharp N-S rainfall gradient exists throughout the region (Figure 1), with annual precipitation values of <500 mm/yr in the north, and increasing to >3000 mm/yr in the south. The source of the precipitation is moisture from the Caribbean, which is carried east to west by the northern branch of the Caribbean low-level jet (Mestas-Nuñez et al., 2002). This results in a slight E-W precipitation gradient, as well. Precipitation values vary seasonally, with the northward migration of the Intertropical Convergence Zone

(ITCZ) resulting in the rainy season during May-October. Southward migration of the ITCZ results in the descending limb of the Hadley cell causing drier conditions throughout the Yucatan. The $\delta^{18}O$ recorded in monthly mean precipitation from the lowland tropics reveals an inverse correlation between the $\delta^{18}O$ and amount of precipitation, meaning that an increase in $\delta^{18}O$ values correlates with a decrease in precipitation. This inverse correlation reflects the "amount effect" described by Rozanski et al. (1993), and is characteristic of lowland tropical regions with highly convective rainfall.

The Maya Lowlands are an excellent location for speleothem paleoclimatology studies because of the numerous caves. The geology of the Maya Lowlands is characterized by limestone bedrock dominated by karst features. A total of thirteen caves were visited in August 2006, and speleothems from two caves were selected for this study (Figure 1). Cueva Tzabnah (Tecoh speleothem) is located in a region known as the northern pitted karst plain (Weidie, 1985), characterized by a thin layer of Cenozoic carbonates overlying older karstified Cretaceous limestones. Cueva Columnas (Hobo 5 speleothem) is located along the southeastern portion of the Ticul fault zone, a WNW-trending escarpment about 100km long (Perry et al., 2002), developed in Tertiary and Cretaceous limestones. The Yucatan is characterized by rapid infiltration of precipitation (Perry et al., 2002), related to the extensive karst development in the limestone bedrock. The relatively short residences time of groundwater means that the isotopic values of drip water entering the cave environment should be at or near the isotopic values of the precipitation (Perry et al., 2002).

Typically, tall cylindrical stalagmites are used in paleoclimate studies, as they are composed of a sequence of superimposed layers, resulting in a continuous growth record (White, 2004). Precipitation of speleothem calcite occurs when rainfall percolates through soil and dissolves CO_2, resulting in acidic water that then dissolves $CaCO_3$ as it infiltrates the limestone bedrock. The amount of $CaCO_3$ dissolution is dependent upon the pCO_2 of the soil. Eventually the water becomes saturated with $CaCO_3$, and when it reaches the cave environment, it is out of equilibrium with the environment. The CO_2 degasses, resulting in the drip water becoming supersaturated with $CaCO_3$, which then precipitates as speleothem calcite (White, 2004). Calcite deposition and speleothem growth rate is primarily dependent upon $[Ca^{2+}]$ of the drip water (Turgeon and Lundborg, 2003).

Previous Climate Studies in the Maya Lowlands

The major objective of this study is to constrain the timing of droughts that may have played a role in Maya cultural evolution during the late terminal Classic Period (ca. 800-1050 AD). Prior lake studies (Curtis et al., 1998; Hodell et al., 1995; Rosenmeier et al., 2002) provide evidence for extended periods of regional drought in the Yucatan Peninsula during the terminal Classic Period. The hypothesis that climate change is linked to the collapse of the Maya is controversial, partly because the timing and duration of the drought events is not well-constrained in the lake records. Lake studies from this region rely heavily upon ^{14}C dating methods. Radiocarbon dates need to be calibrated in order to correct for variations in the rate of atmospheric ^{14}C production, and the Intcal calibration curve yields multiple ages for three different time periods during the Terminal

Classic. This ambiguity makes it extremely difficult to determine the exact timing or duration of drought events recorded in lakes during the terminal Classic.

Several climate studies using lake sediment cores have characterized climate conditions in the Yucatan on the scale of thousands or tens of thousands of years (Leyden, 2002, Leyden et al., 1994, Rosenmeier et al., 2002). The climate archives from numerous lakes in the Maya Lowlands reveal evidence for drought during the terminal Classic Period, dated using ^{14}C. The evidence for drought includes changes in the palynological assemblages, variations in $\delta^{18}O$ as measured in gastropods and ostracods, changes in density of lake sediments, paleoshoreline features indicating water level drops, and changes in gastropod assemblages. The $\delta^{18}O$ values recorded in these tropical closed-basin lakes is controlled by the ratio of evaporation to precipitation, because of the preferential loss of ^{16}O during evaporation, thereby increasing the $\delta^{18}O$ during times of low precipitation (Hodell et al., 2001). However, from about 4200 years ago to about 1000 ^{14}C yr BP, Maya land use patterns altered the climate signals recorded in the lake records (Curtis et al., 1998). Evidence exists for extensive forest clear cutting and increased soil erosion in the Maya Lowlands in the Peten lake district in Guatemala during the late Holocene, which would alter both the $\delta^{18}O$ (due to changes in the hydrologic budget of the watershed), as well as the palynological assemblages recorded in lake sediments (Curtis et al., 1998). These Maya land use practices make interpretation of the $\delta^{18}O$ record difficult in some areas. Despite these difficulties in the Peten, well-established drought events during the terminal Classic are recorded in Lake Chichancanab in north central Yucatan, and Lake Punta Laguna, in eastern Yucatan.

In Lake Chichancanab (Figure 1), changes in oxygen isotopes and gypsum precipitation are used to reconstruct the climate of the Yucatan over the last 2600 years (Hodell et al., 2001). Gypsum precipitation, measured as weight percent total sulfur, is used as a proxy for drier climate conditions because as the evaporation to precipitation ratio increases, the lake volume decreases, resulting in supersaturation of $CaSO_4$ and precipitation of gypsum. This lithologic proxy reveals three dry periods where gypsum dominates the lake sediments: 475-250 BC (2425-2200 yr BP), 125-210 AD (1825-1740 yr BP), and 750-1025 AD (1200-925 yr BP) (Figure 2). The most recent of those three drought periods was longer in duration and spans the terminal Classic (Hodell et al., 2001). There are also two distinct drought events within the dry period, occurring at 800 AD (1150 yr BP) and 1020 AD (930 yr BP). $\delta^{18}O$ values are also above the average value between 800 and 1090 AD. The overall drought events contained in the gypsum and $\delta^{18}O$ record from Lake Chichancanab also reveal a 208-year periodicity, which has been attributed to solar forcing because it corresponds with a 206-year cycle in the production of cosmogenic nuclides (Hodell et al., 2001).

The $\delta^{18}O$ recorded in gastropods and ostracods in lake sediments from Lake Punta Laguna (Figure 1) also reveal a dry period from 165-1020 AD (1785-930 yr BP), with three distinct and especially dry events at 862, 986, and 1051 AD (1171, 1019, and 943 yr BP; Curtis et al., 1996) (Figure 2). The $\delta^{18}O$ values decrease after 930 yr BP, indicating a return to wetter conditions after the terminal Classic period (Curtis et al., 1996). Another drought event is also recorded by an increase in the $\delta^{18}O$ values at 1391 AD (559 yr BP).

In addition to records of drought events occurring in the terminal Classic, regional lakes also reveal evidence for drought events in the last 1000 years of the Holocene. In the northwestern Yucatan, a study of lake sediments from Aguada X'caamal (Figure 1) contains climate data from the past 2600 years (Hodell et al., 2005). The $\delta^{18}O$ values recorded in ostracods, gastropods, and carbonate-encrusted stems of charophytes indicate drier conditions on the Yucatan Peninsula during the Little Ice Age (Figure 2). The $\delta^{18}O$ values of the three organisms increase an average of 2.2‰ between 1400 and 1500 AD, indicating drier conditions persisted in the Yucatan (Hodell et al., 2005). This increase in $\delta^{18}O$ values is also mirrored in the $\delta^{18}O$ records from Lake Chichancanab (Hodell et al., 1995) and Lake Salpeten in the Maya Lowlands of Guatemala (Rosenmeier et al., 2002), indicating regional drying during the 15th century AD.

In order to replicate the drought events recorded in regional lakes, and to obtain a more accurate chronology, speleothems from the Yucatan are used in this study. Spelothems provide a recent record of climate from the last 2 to 3 thousand years at a higher resolution (sub-decadal). The ability to date speleothems using U/Th techniques allows for more accurate dating than ^{14}C dating of lake sediment cores, due to the problems associated with ^{14}C dating. U/Th dating of speleothems can yield precise and accurate dates of numerous growth layers along the growth axis of the speleothem and do not require calibration (Dorale et al., 2004). These dates will allow for accurate dating of climate events as recorded in the $\delta^{18}O$ and for correlation with other records from the region.

The $\delta^{18}O$ from speleothem calcite is a proxy for changes in the $\delta^{18}O$ of past precipitation, which are caused by the N-S migration of the ITCZ. The speleothem $\delta^{18}O$ can be an accurate proxy for changing climate and the prevalence of droughts during the last 2 to 3 thousand years. Because the $\delta^{18}O$ of lakes is a measure of the ratio of evaporation to precipitation, it can be affected by anthropogenic land use patterns within a lake's watershed. Therefore, the $\delta^{18}O$ records from speleothems will have the potential to provide a clearer picture of the occurrence of drought-related climate events in the late Holocene, and the U/Th dates will be able to constrain the timing and duration of these events. This will allow researchers to better evaluate the role that drought may have played in the collapse of the Maya during the terminal Classic Period.

Paleoclimate Reconstructions Using Speleothems

Because of their nature of formation, speleothems are very useful for inferring paleoclimate and dating past climate events. The continuous formation of growth layers depends on a steady supply of drip water, and hiatuses in the growth can be used to infer drier climate conditions. The isotopic composition of the speleothem calcite is controlled by the isotopic composition of the drip water, the ambient cave temperature, and the relative humidity of the cave, and can be used as a proxy for the isotopic composition of past precipitation.

The isotopic composition of the drip water percolating into the cave is controlled by several factors. Initially, water evaporating from the ocean surface will have a particular isotopic composition, $\delta^{18}O_{sw}$, which can also be affected by the temperature of seawater evaporation. The transport of the water vapor to the cave site can alter the isotopic composition as well, due to variable storm tracks and "rainout" of the heavier ^{18}O isotope. Once the precipitation infiltrates the soil, it can be affected by processes within the soil horizon as well as interactions with seepage water within the epikarst (Harmon, et al., 2004). Over the time scale of this study, we assume these factors have remained fairly constant. The resulting $\delta^{18}O_{dw}$ (drip water) is thus a function of the isotopic composition of the rainfall ($\delta^{18}O_{pptn}$), which is largely influenced by the amount of precipitation, i.e. the "amount effect" (Rozanski, et al., 1993). This results in an inverse correlation between amount of precipiation and $\delta^{18}O$ values, such that an increase in precipitation will result in a decrease in $\delta^{18}O$ values. The resulting isotopic composition of the speleothem calcite ($\delta^{18}O_c$) can then be used as a proxy for the isotopic composition of past precipitation.

In order to use $\delta^{18}O$ values from speleothem calcite to infer past climate conditions, the calcite must be deposited in isotopic equilibrium with the drip water. The $\delta^{18}O$ values recorded in speleothems are impacted by temperature, the $\delta^{18}O$ values of the drip water, and evaporation (Harmon et al., 2004). Speleothems growing in the interior of caves with high humidity and stable temperatures are the most likely to be deposited in isotopic equilibrium, because the effects of temperature and evaporation are minimized. Speleothems collected for this study were all collected from interior cave passages in order to minimize these evaporative effects. Therefore, the $\delta^{18}O$ of the speleothem calcite should be an accurate reflection of the $\delta^{18}O$ of the drip water, which we assume is representative of the $\delta^{18}O$ of past precipitation. Because the $\delta^{18}O$ of rainfall changes as a function of climate conditions, and because it has a negative correlation with the amount of rainfall in tropical lowland areas, the $\delta^{18}O$ of the speleothem calcite is a useful proxy for variations in past precipitation in the Maya Lowlands.

Dating Speleothems Using U/Th Disequilibrium Methods

Speleothem calcite is datable using U/Th methods because the highly-soluble uranyl ion (UO_2^{2+}) is easily carried by the drip water, whereas the very insoluble Th^{4+} is not. This results in uranium being incorporated in the speleothem calcite, and creates conditions where the initial amount of the daughter ^{230}Th is assumed to be very low. The decay of the ^{238}U parent to the daughter ^{230}Th isotope is part of the ^{238}U decay chain, and the ingrowth of ^{230}Th in the speleothem calcite allows for the use of the U/Th geochronometer to accurately and precisely date the growth layers (Edwards et al., 1987). The smaller the amount of detrital ^{230}Th that is incorporated into the speleothem calcite, the higher the parent to daughter ratio is, and the better the speleothem calcite can be used for dating.

Speleothem calcite has been successfully dated using U/Th techniques since the first mass spectrometric measurements were made on speleothems in 1989 (Li et al., 1989). Since then, improvements have been made in the ability to measure U and Th isotopes using inductively-coupled plasma mass spectrometers (ICP-MS; Shen et al., 2002), and U/Th dating has been used to obtain accurate and precise dates on numerous speleothems, ranging in age from tens of years to up to 600,000 years old (Dorale et al., 2004). The ability to date the growth layers of the speleothem calcite means that the timing of the climate events contained in the isotopic records can be constrained. An accurately dated climate record can then be used for comparison with other climate records in order to interpret regional versus global climate patterns, as well as to determine the possible cyclicity of climate events.

METHODS

Field methods

Fourteen speleothem specimens were collected from 7 caves in the Yucatan peninsula in the summer of 2006. The Hobo 5 speleothem was collected during the 2004 field season. Speleothem collection procedures followed guidelines established by the National Speleological Society, recognizing the need to conserve and protect cave environments. Cylindrical columnar stalagmites, most likely to contain a continuous stratigraphy, were collected from the interior of the caves to minimize any evaporation effects. When possible, stalagmites growing under active drip water were chosen.

Analytical methods

Stable isotopes

Light stable isotope analyses were conducted at the Stable Isotope Mass Spectrometry Lab in the Department of Geological Sciences at the University of Florida. Each stalagmite was halved along the growth axis, and one half polished and used for stable isotope sampling. Samples were milled using a Sherline 5100 vertical mill with a

0.02 mm drill bit at 0.5 mm intervals along the entire growth axis, yielding 478 samples. A series of samples was also drilled along a growth layer at 80 mm in order to perform a Hendy test to check for deposition of calcite in isotopic equilibrium with the dripwater. Samples weighing 70-100 μg were loaded into a VG/Micromass (now GV Instruments) PRISM Series II isotope ratio mass spectrometer with an Isocarb common acid bath preparation device. Stable isotopes of carbon and oxygen were measured by converting them to CO_2 by reacting them with phosphoric acid at 70°C. Standards were run every 18 samples, using the NBS-19 standard. Precision is better than 0.1‰ for both carbon and oxygen. Values are reported in per mil relative to V-PDB.

U/Th dating

Initially, the base of each speleothem collected was dated in order to determine maximum ages for each. The tops of six different speleothems were then dated to identify a speleothem with a growth period that spanned the late Holocene. Based on these preliminary data, the speleothem Tecoh was chosen for additional dating. Twenty-three subsamples from Tecoh were selected for U/Th dating, and fourteen subsamples were selected from Hobo 5. Most of the subsampling took place in Duluth, following procedures designed to minimize contamination of the samples, with the exception of two subsamples from Tecoh and seven subsamples from Hobo 5, which were drilled out at the University of Florida. All chemical procedures were conducted in a clean lab setting. The speleothem was first ultrasonicated to remove any potential sources of contamination on the speleothem surface. Growth layers, chosen based on the quality of the calcite and their relative position on the growth axis, were sub-sampled using a Dremel-type drill with a carbide tip cleaned using 0.1N HCl and then methanol. Chemical isolation of U and Th isotopes was performed following procedures outlined by Edwards, et al. (1987) and outlined in Appendix 1.

The samples were analyzed at the Minnesota Isotope Lab on the Twin Cities campus of the University of Minnesota. Chemical separates for U and Th were run on the Finnigan Element ICP-MS using the multiplier in ion-counting mode (Shen et al., 2002), using a standard U solution (112a) of known isotopic composition. These measurements were then used in the $^{230}Th/^{238}U$ decay equation in order to determine the age of the samples.

RESULTS

Sample descriptions

One speleothem spanning the late Holocene from Cueva Tzabnah in Tecoh, Mexico (N20°43.810' W89°28.462', Figure 1) was selected for further study. Prior to its collection during the 2006 field season, the speleothem "Tecoh" had been broken by vandalism, most likely within the last ten years, and was not discovered in situ. Discussions with the cave owner indicate the speleothem originated from an interior passage of the cave (see Appendix 2), which was then visited by the field party. The Tecoh speleothem is 25 cm in length and ranges from 8 cm wide at its base, narrowing to about 4.5 cm near the top. It exhibits visible growth laminations ranging in color from clean to white to cream colored calcite, as well as several darker colored layers, most likely due to the incorporation of humic matter transported from the surface (Figure 3). Hiatuses are visible at 65-68 mm and 71.5-76 mm, where there are layers of what appear to be biological growth on the surface of the speleothem, consisting of tubular structures about 0.01 mm in diameter (Figure 3). There are also other dark layers at 35 mm, 105 mm, and 144.5 mm.

The Tecoh speleothem is also compared to another late Holocene speleothem, Hobo 5 from Cueva Columnas, located at Rancho Hobonil (Figure 1) near Tzucacab, Mexico, collected during the 2004 field season. Hobo 5 was collected from an interior passage of the cave (see Appendix 3). Hobo 5 is 22 cm long and about 4.5 cm wide. The growth layers are highly variable, ranging from clear to white to gray to brown in color, and vary in thickness (Figure 4).

U/Th Dating and Speleothem Age Models

Twenty-three ^{230}Th ages were obtained from the Tecoh speleothem (Table 1). Decay constants used in the $^{230}Th/^{238}U$ age equation are shown in Table 1. Concentrations of ^{238}U range from 119-553 ppb. Because ^{230}Th was incorporated with the detrital ^{232}Th component, ages were corrected using an initial $^{230}Th/^{232}Th$ atomic ratio of $(4.4 \pm 2.2) \times 10^{-6}$, assuming an error of ±50%, which is the value for a material at secular equilibrium, with the bulk earth $^{232}Th/^{238}U$ value of 3.8. Dates are reported with 2σ analytical errors that average ±77 yr and range between ±21 and ±329 yr. I regard thirteen of the original twenty-three dates from Tecoh as reliable. Three of the unreliable dates were likely affected by contamination by material from nearby dirty layers that was incorporated during subsampling (Te-12, Te-38, and Te-70. Five other dates (Te-136, Te-140, Te-173, Te-182, and Te-243) are suspect because the subsample location included dissolution pits within the speleothem calcite. The presence of dissolution pits at these locations indicates an open system environment, allowing the remobilization of uranium, thus yielding invalid dates. The top and basal dates (Te-T and Te-B) were also deemed unreliable. The relatively higher ^{232}Th and the relatively older ages of these samples indicate they were likely contaminated by older material during subsampling. The reliable dates indicate Tecoh has a maximum age of 1240 ±61 yr BP and a minimum age of 200 ±61 yr BP, and an average error of ±51 yrs.

All ages are in stratigraphic order or within quoted uncertainties (Figure 5). Based on the available dates as well as the morphology of the speleothem, Tecoh experienced two distinct intervals of growth, separated by a hiatus between 65 and 75 mm, which lasted for 160 years. Although there is a thin growth layer at 69 and 71.5 mm, it was not possible to get a date from that location in order to constrain the timing of this short interval of growth. For the lower portion of the speleothem (75-246 mm), individual ages for each $\delta^{18}O$ value were interpolated using a third order polynomial (Figure 6). For the upper portion (0-65 mm), a second order polynomial was used to interpolate individual ages for each $\delta^{18}O$ (Figure 7). The average error of the samples used to create the age model is shown for reference by vertical error bars to the right of the $\delta^{18}O$ curve on Figure 11.

Using the above chronology, growth rates along the axis of the Tecoh speleothem exhibit a dramatic change between the upper and lower portions of the speleothem. The upper 65 mm grew for 630 years. The growth rate ranged from 0.12 mm/yr to 0.05 mm/yr with an average growth rate of 0.10 mm/yr. The lower 75-246 mm grew for 501 years. The growth rate ranged from 2.38 mm/yr to 0.14 mm/yr, with an average growth rate of 0.34 mm/yr. The higher growth rate for the lower portion results in a higher resolution oxygen isotopic record, which has a sampling interval of 0.5 mm.

Fourteen ^{230}Th ages were obtained from the Hobo 5 speleothem (Table 2). Concentrations of ^{238}U range from 97-258 ppb. Ages were corrected using an initial ^{230}Th/^{232}Th atomic ratio of $(4.4 \pm 2.2)\times10^{-6}$ and dates are reported with 2σ analytical errors that average ±214 yr and range between ±31 and ±1031 yr. I regard seven of the original fourteen dates from Hobo 5 as reliable. One of the unreliable dates is likely related to problems encountered during lab chemistry (H5-32). Another sample contained detrital material from nearby dirty layers (H5-141). Five other dates have uncertainties that are too large to make the ages meaningful (H5-110, H5-126, H5-135, H5-149, and H5-183). After using the remaining date to construct the age model, Hobo 5 has a maximum age of 1347 ±63 yr BP and a minimum age of 520 ±99 yr BP, and an average error of ±89 yrs.

All ages used to establish the age model are in stratigraphic order (Figure 8). Linear interpolation between points and extrapolation beyond points was used to interpolate individual ages for each δ^{18}O value (Figure 8); polynomial fit lines provided no improvement to the age model. Using this age model, growth rates along the axis of the Hobo 5 speleothem range from 1.25 mm/yr to 0.07 mm/yr, with an average growth rate of 0.23 mm/yr. The speleothem grew for 849 years, from 603-1452 AD.

$\delta^{18}O$ Results

Tecoh

Four samples of drip waters from Cueva Tzabnah were collected during the 2005 and 2006 field seasons, and have an average $\delta^{18}O$ value of –3.40‰. This value is close to the regional precipitation value of –3.91‰ as well as the groundwater value of –3.92‰ from Punta Laguna (Curtis et al., 1996).

In order to test for kinetic isotopic fractionation, a Hendy test (Hendy, 1971) was performed on Tecoh along a single growth layer located at 81 mm (Figure 9). In order to demonstrate that deposition of calcite has occurred in isotopic equilibrium, the range of $\delta^{18}O$ values should be <0.80‰, and the progressive enrichment of $\delta^{13}C$ with distance from the central growth axis should not be greater than twice the enrichment of $\delta^{18}O$ along the same distance. The variation in $\delta^{18}O$ within the layer is <0.60‰, and although the $\delta^{18}O$ and $\delta^{13}C$ values covary, they do not show progressive enrichment with increasing distance from the central growth axis (Figure 9). Also, a plot of the $\delta^{18}O$ and $\delta^{13}C$ values along the entire growth axis show a low degree of correlation ($r^2 = 0.20$) (Figure 9). These data suggest that the conditions for deposition of calcite in isotopic equilibrium have been met.

Oxygen isotope data were filtered using a 5-point running mean (Figure 10). The $\delta^{18}O$ values range from –2.46‰ to –6.65‰, with a mean value of –5.25‰. The $\delta^{18}O$ of the upper 65 mm is isotopically heavier, with a mean value of –4.95‰, whereas the lower 75-246 mm is isotopically lighter, with a mean value of –5.36‰.

In the lower 75-246 mm, isotopic values decrease from the mean value from 722-854 AD, followed by periods from 854-914 AD where the values increase from the mean value, with the exception of a short interval between 880-886 AD where the values decrease again. Between 914-966 AD, $\delta^{18}O$ values decrease from the mean, followed by a time period from 966-995 AD, where values fluctuate above and below the mean. Isotopic values then decrease from the mean from 995-1142 AD, then begin to increase from the mean value again from 1142-1223 AD, leading into the prominent hiatus at 75 mm. In the upper 65 mm of the speleothem, $\delta^{18}O$ values decrease from the mean between 1381-1539 AD, and then begin to increase, staying heavier than the mean from 1603 AD to the present.

Hobo 5

Nine samples of drip waters from Cueva Columnas were collected during the 2005 and 2006 field seasons and have an average $\delta^{18}O$ value of –2.26‰. Samples of rainwater collected at Rancho Hobonil from 8/12/06-1/5/07 have an average $\delta^{18}O$ value of –1.05‰. The difference in isotopic values could reflect seasonal isotopic variations. During the winter, the ITCZ shifts to the south, precipitation decreases, and the $\delta^{18}O$ value of precipitation increases. Drip water samples collected during the summer field season would be expected to be isotopically lighter than the precipitation samples collected during the winter, which is observed.

Oxygen isotope data were filtered using a 5-point running mean (Figure 11). The $\delta^{18}O$ values range from –2.95‰ to –4.54‰, with a mean value of –3.80‰. There are three distinct time periods with different isotopic signatures. From 603-897 AD, $\delta^{18}O$ values increase above the mean value. From 897-1392 AD, $\delta^{18}O$ values decrease below the mean value. From 1392-1452, $\delta^{18}O$ values fluctuate above and below the mean value.

DISCUSSION

Because of the "amount effect" that influences the $\delta^{18}O$ value of precipitation in lowland tropical areas, and because speleothem $\delta^{18}O$ is a proxy for the $\delta^{18}O$ of past precipitation, speleothem $\delta^{18}O$ values heavier than the mean are interpreted as relatively drier climate periods with less precipitation and vice versa. The $\delta^{18}O$ data and hiatuses in speleothem growth suggest the Yucatan experienced several dry periods during the late Holocene. In this discussion, I will compare the nominal timing (since error bars vary) of wetter and drier events in Tecoh, Hobo 5, the three relevant lake records from the Yucatan, and the Cariaco Basin record. After the detailed comparison, I will include an error analysis and evaluate what broad trends can be supported by the data.

Evidence from the Tecoh speleothem reveals the occurrence of three relatively drier periods from 854-914 AD, 1142-1381 AD, and from the 17th century to the present. The earliest of these events is preceded by a relatively wetter period, where the mean $\delta^{18}O$ value for 738-854 AD is 0.32‰ lighter than the mean speleothem value (Figure 12). From 854-914 AD, the mean $\delta^{18}O$ value is 0.37‰ heavier than the mean speleothem value. Within this period, there are two peak dry events centered at 874 AD and 907 AD, and another less intense event at 894 AD. The Hobo 5 speleothem indicates the existence of a long relatively dry period spanning 603-897 AD, with an increase in the mean value of 0.23‰ over the mean speleothem value. Within that time period, the most intense dry event lasted from 834-897 AD, with the peak centered at 871 AD.

These relatively dry periods recorded in Tecoh and Hobo 5 corresponds with a drought recorded in the $\delta^{18}O$ record from Punta Laguna, 140 km east of Cueva Tzabnah and 150 km northeast of Cueva Columnas (Figure 12), which occurred from 830-890 AD, with a peak at 850-860 AD (Curtis et al., 1996; Hodell et al., 2007). The relative timing of the Punta Laguna and Tecoh drought events cannot be resolved, as they are within error of each other, however, the duration of the dry period is roughly the same at about sixty years. This time period also corresponds with archeological evidence indicating the northern Yucatan experienced cultural collapse from 861-910 AD (Gill, 2000). The $\delta^{18}O$ record from Aguada X'caamal, about 10 km to the west of Cueva Tzabnah, and about 85 km northwest of Cueva Columnas, indicates a dry period from 825-850 AD (Hodell et al., 2005). Although this dry period slightly predates the one recorded in the Tecoh speleothem, its date is not well constrained. The closest radiocarbon date, 1116 cal yr BP, has a 2σ error of ± 105. At Lake Chichancanab, 120 km southeast of Cueva Tzabnah, and about 35 km southeast of Cueva Columnas, there is evidence for an extended drought from 800-1000 AD, with the peak occurring at 922 AD. Although this drought is longer in extent, its duration encompasses the timing of the dry periods recorded in both the Tecoh and Hobo 5 $\delta^{18}O$ records. These correlations indicate that although the region experienced drier climate conditions from 800-1000 AD, the drought occurred later and was shorter in duration in the northern Yucatan.

After the relatively dry period recorded in Hobo 5 from 603-897 AD, the $\delta^{18}O$ record indicates climate conditions became relatively wetter from 897-1392 AD (Figure 12). During this time period, the mean $\delta^{18}O$ value was 0.19‰ lighter than the mean speleothem value. After 1392 AD, the $\delta^{18}O$ record fluctuates, with a mean $\delta^{18}O$ value of 0.08‰ heavier than the mean speleothem value, until the speleothem ceased growing at 1452 AD.

After the relatively dry event recorded in the Tecoh speleothem from 854-914 AD, climate began to fluctuate, with several wet/dry cycles evident in the Tecoh $\delta^{18}O$ record, during the time period from 914-1142 AD. This time period has an average $\delta^{18}O$ value that is 0.17‰ lighter than the mean. After this time period, a second relatively dry event is evident from 1142-1381 AD. During the drier period from 1142-1223 AD, the mean $\delta^{18}O$ is 0.32‰ heavier than the mean speleothem value. After 1223 AD, there is an extended hiatus. Within the hiatus, there is a thin, 2.5 mm layer of calcite. $\delta^{18}O$ values for this region are 0.35‰ heavier than the mean. For this second relatively dry period recorded in Tecoh, correlations are less clear. The Punta Laguna record contains evidence for a relatively drier period from 1225-1299 AD (Curtis et al., 1996). Aguada X'caamal also shows a dry period beginning around 1290 AD, which increases in intensity during the 15th century. Hodell et al. (2005) attribute this to cooling associated with the Little Ice Age.

After the 158-year long hiatus, there is an extended relatively wet period from 1381-1539AD, where the mean $\delta^{18}O$ value is 0.47‰ lighter than the mean speleothem value (Figure 13). Beginning in 1602 AD, climate begins to dry again, and stays relatively dry until the present. 1602 AD to present has an average $\delta^{18}O$ value is 0.58‰ heavier than the mean speleothem value. This relatively dry period correlates with the $\delta^{18}O$ record from Aguada X'caamal, which stays heavier throughout the late Holocene until the present. The authors have interpreted the heavier values as a signal of a drying climate or a change in basin hydrology. Climate conditions have increasingly become drier on the northern Yucatan peninsula over this time period. Archeological records also indicate cold and famine existed on the Yucatan during the Little Ice Age, recorded in the Book of Chilam Balam, a Maya text (Gill, 2000).

It is also possible to compare the $\delta^{18}O$ records from Tecoh and Hobo 5 to regional records, such as the climate archive contained in the sediments of the Cariaco Basin of the southern Caribbean. The Yucatan peninsula and northern South America are similarly affected by seasonal as well as longer-term variations in the position of the Intertropical Convergence Zone. Haug et al. (2003) details a series of drought events recorded in the sediments of the Cariaco Basin, as reflected in the bulk Titanium content, indicative of riverine input to the basin. Higher Titanium content reflects greater riverine input, and is interpreted as a proxy for increased precipitation. Titanium minima are recorded at 760, 810, 860, and 910 AD (±30 years), and are interpreted as the beginning of multiyear drought events (Haug et al., 2003), caused by a more southerly position of the ITCZ. The latter two events fall within the dry period recorded in Tecoh from 852-914 AD, and the 860 AD event falls within the peak dry period from 834-897 AD recorded in the Hobo 5 record. The Ti record indicates the 860 AD event lasted ~3 years, and the 910 event lasted ~6 years. Another correlation between the Cariaco and the Tecoh records is the simultaneous climate shift that occurs during the last 500 years, where climate drying is interpreted from low Titanium values in the Cariaco Basin and increased $\delta^{18}O$ values in the Tecoh speleothem.

Although it is easy to make correlation between the speleothem isotope data and existing lake records, it is necessary to take into consideration the error values associated with each record. The error associated with the speleothem records, ±51 yrs for Tecoh, and ±89 yrs for Hobo 5, means that it is difficult to resolve the timing of climate events, and also limit the ability to correlate with other records which each have their own associated error values. Of the records presented for correlation in this study, the Cariaco Basin record is the best constrained, with an average error value of ±30 yrs. It is important to note that the timing of the drier climate events within the more precise Cariaco record support the timing and existence of the relatively drier events recorded in the speleothem isotope records.

A possible mechanism for changing climate in the Maya Lowlands is a shift in the mean position of the ITCZ during the late Holocene. It should be possible to quantify the variation in the $\delta^{18}O$ of precipitation (and hence speleothem $\delta^{18}O$) as a function of latitudinal shift of the ITCZ. Knowing this would allow researchers to estimate the approximate latitudinal shift in the mean position of the ITCZ given an increase or decrease in $\delta^{18}O$ values. However, no long-term data of stable isotope values in precipitation exist for the Yucatan Peninsula. Data do exist for the International Atomic Energy Agency (IAEA) station in Veracruz, Mexico. Although Veracruz is not located in the Yucatan, it is at a similar latitude at 19.2°N.

In order to estimate the approximate southerly shift in the mean position of the ITCZ required to produce the variation in $\delta^{18}O$ values observed in the Tecoh and Hobo 5 speleothems, I used the mean monthly $\delta^{18}O$ values measured in precipitation at Veracruz, recorded since 1962. Because the seasonal migration of the ITCZ is fairly well known for recent times, I took the difference in the mean $\delta^{18}O$ in precipitation between January and July, and used the difference in the mean latitudinal position of the ITCZ between January and July to establish a gradient of change in $\delta^{18}O$ per degree latitude. I then applied this gradient to the variation seen in the speleothem $\delta^{18}O$ records. Based on the estimated gradient of 0.15‰ per degree latitude, it is possible to estimate about a 2° shift to the south in the mean position of the ITCZ during the drought recorded in the Tecoh speleothem from 854-914 AD. This southerly shift of the ITCZ would lead to drier conditions persisting in the region. The drying observed in the Tecoh speleothem from 1602 AD to present would correlate with about a 4° southerly shift in the mean position of the ITCZ. The three relatively wetter periods observed in the Tecoh record (738-854 AD, 914-966 AD, and 995-1142 AD) would correlate with about a 2° northerly shift in the mean position of the ITCZ.

Another way to estimate the magnitude of past precipitation change is to determine the gradient between $\delta^{18}O$ per precipitation amount. Using the data for annual precipitation from the IAEA Veracruz station, the $\delta^{18}O$/precipitation amount gradient is –1.94‰ per 1000 mm precipitation. Applying this gradient to the Tecoh oxygen isotope record, it is possible to estimate a relative decrease in the mean annual precipitation of

784 mm/yr from the peak of the relatively wetter period from 738-854 AD (centered at 830 AD) to the peak of the relatively drier period from 854-914 AD (centered at 874 AD). Although this is simply a crude estimate, it represents a significant decrease in mean annual precipitation. The modern value for mean annual precipitation is about 1000 mm/yr. Using the modern values for mean annual precipitation and for the oxygen isotopic values, this means that the mean annual precipitation for wettest periods recorded in the Tecoh speleothem is about 1700 mm/yr greater than modern precipitation.

CONCLUSIONS

The paleoclimate record from the $\delta^{18}O$ of the Tecoh and Hobo 5 speleothems provides additional evidence to support the occurrence of regional droughts on the Yucatan Peninsula during the late Holocene, including dry periods that coincide with Maya cultural collapse during the Terminal Classic. The observed drought events correlate with regional studies of Yucatan lakes and sediments from the Cariaco Basin of Venezuela that provide evidence for regional drying during the Terminal Classic. The Tecoh speleothem also provides evidence for drying beginning in the 16th century AD until present. Based on the timing and duration of the droughts as inferred from increases in speleothem $\delta^{18}O$ and lake records, climate became drier earlier and stayed drier longer in the southern Maya Lowlands during the Terminal Classic, than did the northern Yucatan Peninsula. The speleothem and paleolimnological data correspond with archeological evidence suggesting Maya sites in the northern Yucatan were abandoned later than the western lowlands and the southeastern lowlands (Gill, 2000).

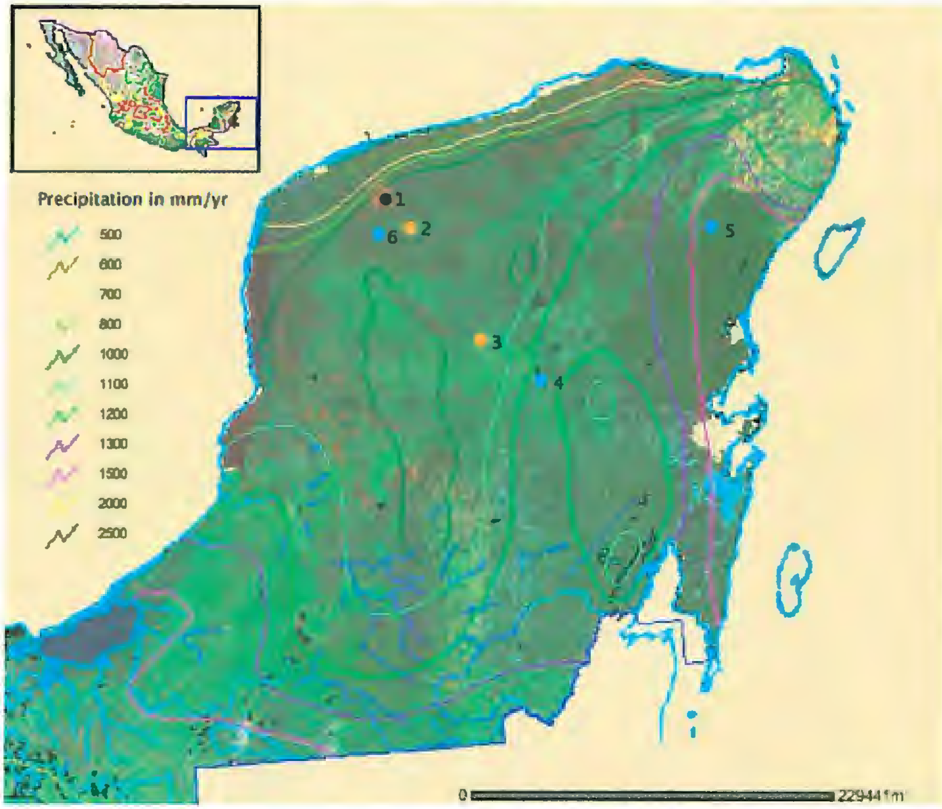

Figure 1. Map of the Yucatan Peninsula showing average annual precipitation (INEGI, 1981). Study locations and places mentioned in the text are shown. In black: 1. Merida; Caves (tan): 2. Cueva Tzabnah, 3. Cueva Columnas; Lakes (blue): 4. Lake Chichancanab, 5. Lake Punta Laguna, 6. Aguada X'caamal.

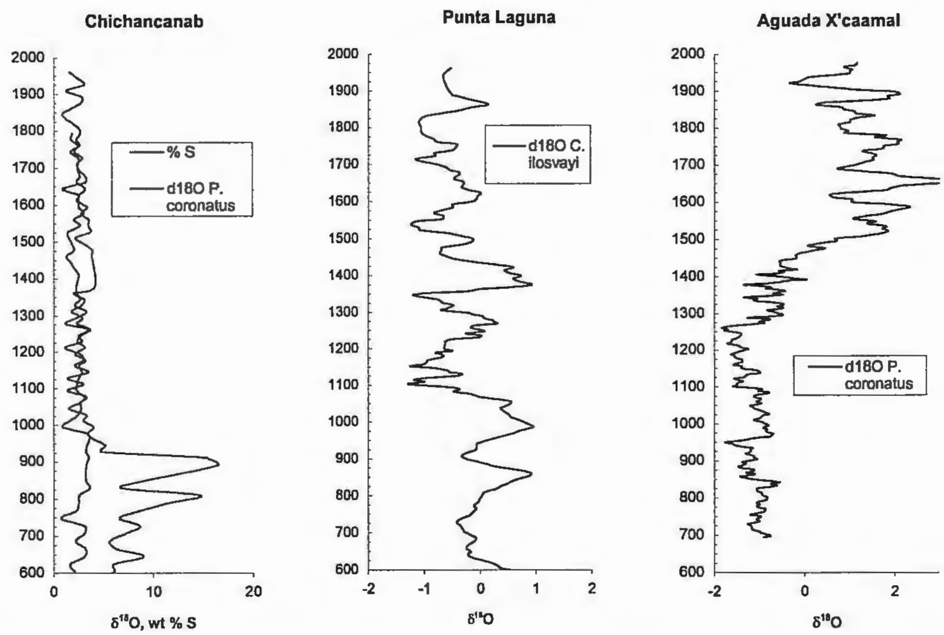

Figure 2. $\delta^{18}O$ data from 600-2000 AD for three Yucatan lakes: Lake Chichancanab, Lake Punta Laguna, and Aguada X'caamal.

Figure 3. A. Photograph of the Tecoh speleothem. B. Close-up of layers with biogenic growth. C. Close-up of an area with dissolution pits, including a sampling location that dissected a dissolution pit. Oxygen isotope sampling track is also visible.

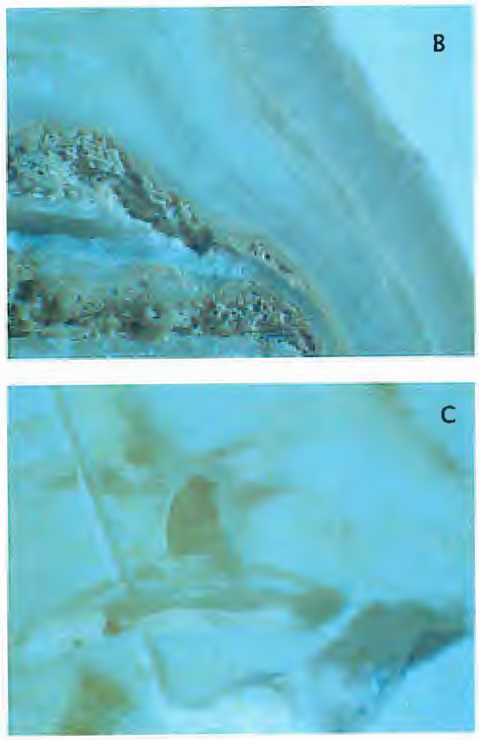

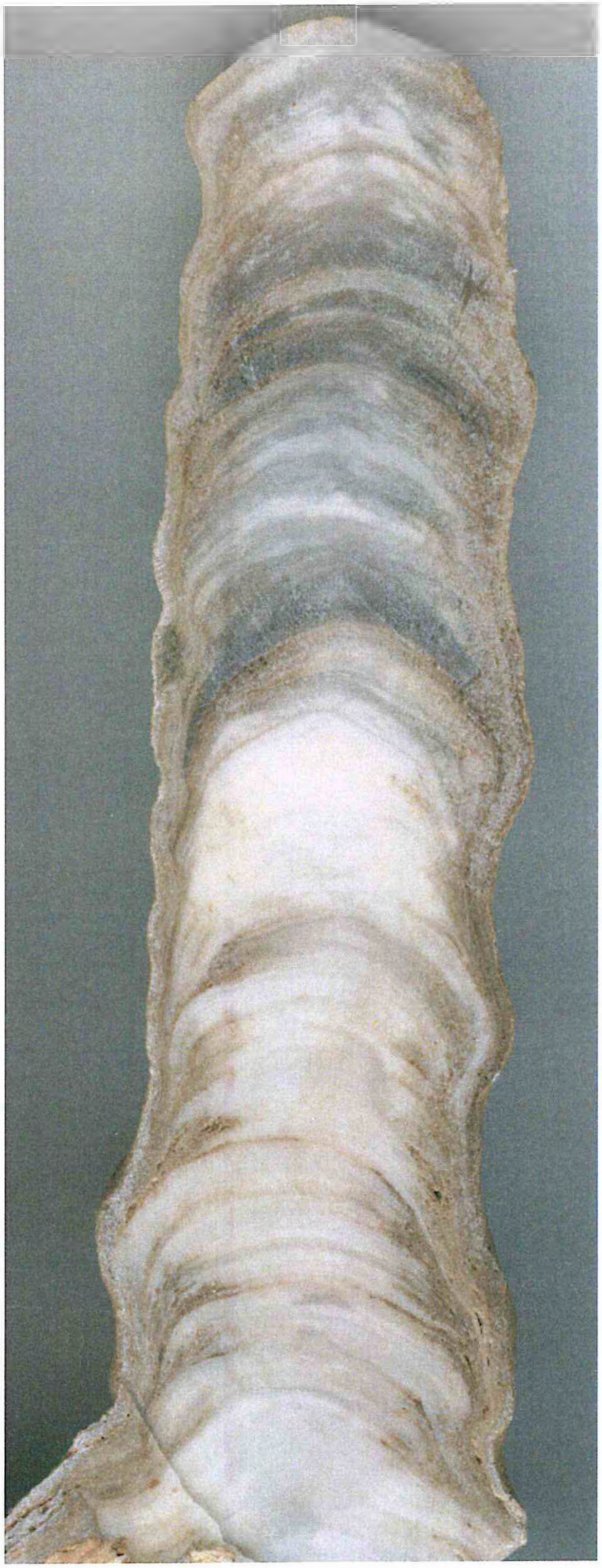

Figure 4. Photograph of Hobo 5 speleothem.

Table 1. Tecoh U/Th dates. Dates used to develop age model are boxed in. The error is 2σ error.

Sample Number	Depth (mm)	^{238}U (ppb)	^{232}Th (ppt)	^{230}Th / ^{232}Th (atomic x10^{-6})	$\delta^{234}U$* (measured)	$^{230}Th/^{238}U$ (activity)	^{230}Th Age (yr) (uncorrected)	^{230}Th Age (yr) (corrected)	$\delta^{234}U_{Initial}$** (corrected)	^{230}Th age (yr BP)*** (corrected)	^{230}Th age (yr AD/BC) (corrected)
TE-T	3	552.9 ±1.4	1579 ± 14	37.5 ±2.6	47.8 ± 2.7	0.00651 ±0.00044	679 ± 46	**599 ± 61**	47.9 ±2.7	**542 ± 61**	**1408 ± 61**
TE-8	8	430.0 ±0.8	56 ± 11	108.5 ±33.4	53.2 ± 2.4	0.00086 ±0.00020	89 ± 20	**85 ± 21**	53.2 ±2.4	**28 ± 21**	**1922 ± 21**
TE-12	12	196.1 ±0.3	599 ± 12	36.9 ±2.4	48.4 ± 2.0	0.00685 ±0.00041	714 ± 43	**629 ± 61**	48.5 ±2.0	**572 ± 61**	**1378 ± 61**
TE-32	32	208.6 ±0.4	126 ± 10	71.7 ±10.3	51.2 ± 2.3	0.00264 ±0.00031	274 ± 33	**257 ± 34**	51.2 ±2.3	**200 ± 34**	**1750 ± 34**
TE-38	38	306.2 ±1.2	453 ± 10	38.6 ±6.9	53.5 ± 5.0	0.00347 ±0.00062	359 ± 64	**318 ± 67**	53.5 ±5.0	**261 ± 67**	**1689 ± 67**
TE-50	50	182.5 ±0.3	100 ± 10	171.3 ±21.6	44.4 ± 2.3	0.00570 ±0.00042	597 ± 44	**581 ± 44**	44.4 ±2.3	**524 ± 44**	**1426 ± 44**
TE-63	63	180.2 ±0.2	133 ± 11	123.9 ±13.9	51.2 ± 1.9	0.00555 ±0.00042	577 ± 43	**557 ± 45**	51.2 ±1.9	**500 ± 45**	**1450 ± 45**
TE-70	70	172.8 ±0.2	2207 ± 13	50.2 ±1.2	44.4 ± 2.0	0.03889 ±0.00089	4,133 ± 97	**3776 ± 203**	44.9 ±2.0	**3719 ± 203**	**-1769 ± 203**
TE-79	79	140.2 ±0.2	124 ± 11	154.0 ±17.4	45.5 ± 2.2	0.00826 ±0.00054	864 ± 57	**839 ± 58**	45.7 ±2.2	**782 ± 58**	**1168 ± 58**
TE-100	100	196.7 ±0.2	148 ± 11	193.2 ±17.4	42.5 ± 1.9	0.00880 ±0.00044	923 ± 46	**902 ± 47**	42.7 ±22.3	**845 ± 47**	**1105 ± 47**
TE-107	107	183.5 ±0.2	43 ± 10	634.1 ±158.7	43.4 ± 1.9	0.00894 ±0.00047	938 ± 49	**931 ± 49**	43.5 ±1.9	**874 ± 49**	**1076 ± 49**
TE-132	132	152.4 ±0.2	45 ± 11	564.0 ±136.9	42.6 ± 2.4	0.00999 ±0.00056	1,049 ± 59	**1041 ± 60**	42.7 ±2.4	**984 ± 60**	**966 ± 60**
TE-136	136	131.2 ±0.2	135 ± 12	177.4 ±17.7	44.3 ± 2.8	0.01106 ±0.00056	1,159 ± 59	**1131 ± 60**	44.4 ±2.8	**1074 ± 60**	**876 ± 60**
TE-140	140	150.3 ±0.2	237 ± 12	152.3 ±9.3	43.4 ± 2.1	0.01456 ±0.00054	1,531 ± 57	**1487 ± 61**	43.6 ±2.1	**1430 ± 61**	**520 ± 61**
TE-148	148	145.5 ±0.2	443 ± 11	58.5 ±3.3	43.8 ± 2.2	0.01081 ±0.00054	1,134 ± 57	**1049 ± 71**	44.0 ±2.2	**992 ± 71**	**958 ± 71**
TE-150	150	156.0 ±0.2	140 ± 11	187.2 ±18.0	43.9 ± 2.4	0.01017 ±0.00051	1,066 ± 54	**1041 ± 56**	44.0 ±2.4	**984 ± 56**	**966 ± 56**
TE-173	173	119.3 ±0.2	155 ± 10	148.9 ±12.5	44.8 ± 2.7	0.01173 ±0.00060	1,230 ± 63	**1193 ± 66**	45.0 ±2.7	**1136 ± 66**	**814 ± 66**
TE-182	182	139.9 ±0.2	1200 ± 12	23.4 ±1.2	42.9 ± 2.6	0.01217 ±0.00062	1,278 ± 66	**1039 ± 137**	43.0 ±2.6	**982 ± 137**	**968 ± 137**
TE-200	200	146.7 ±0.2	66 ± 11	375.4 ±64.7	46.3 ± 2.2	0.01027 ±0.00047	1,074 ± 50	**1062 ± 50**	46.4 ±2.2	**1005 ± 50**	**945 ± 50**
TE-219	219	137.4 ±0.2	173 ± 11	141.3 ±12.3	42.7 ± 2.4	0.01079 ±0.00061	1,133 ± 65	**1098 ± 67**	42.8 ±2.4	**1041 ± 67**	**909 ± 67**
TE-243	243	156.7 ±0.2	241 ± 11	124.1 ±8.2	40.5 ± 2.2	0.01161 ±0.00054	1,222 ± 57	**1179 ± 61**	40.6 ±21.4	**1122 ± 61**	**828 ± 61**
TE-246	246	143.3 ±0.3	125 ± 12	237.2 ±24.9	42.3 ± 2.7	0.01256 ±0.00057	1,321 ± 60	**1297 ± 61**	42.5 ±2.7	**1240 ± 61**	**710 ± 61**
TE-B	base	162.9 ±0.3	3490 ± 14	24.3 ±1.0	42.5 ± 2.8	0.03160 ±0.00125	3,353 ± 135	**2753 ± 329**	42.8 ±2.8	**2696 ± 329**	**-746 ± 329**

$\lambda_{230} = 9.1788 \times 10^{-6}\ y^{-1}$, $\lambda_{234} = 2.8263 \times 10^{-6}\ y^{-1}$, $\lambda_{238} = 1.55125 \times 10^{-10}\ y^{-1}$.

*$\delta^{234}U = ([^{234}U/^{238}U]_{activity} - 1) \times 1000$. ** $\delta^{234}U_{initial}$ was calculated based on ^{230}Th age (T), i.e., $\delta^{234}U_{initial} = \delta^{234}U_{measured} \times e^{\lambda_{234} \times T}$.

Corrected ^{230}Th ages assume the initial $^{230}Th/^{232}Th$ atomic ratio of $4.4 \pm 2.2 \times 10^{-6}$. Those are the values for a material at secular equilibrium, with the bulk earth $^{232}Th/^{238}U$ value of 3.8. The errors are arbitrarily assumed to be 50%.

***B.P. stands for "Before Present" where the "Present" is defined as the year 1950 A.D.

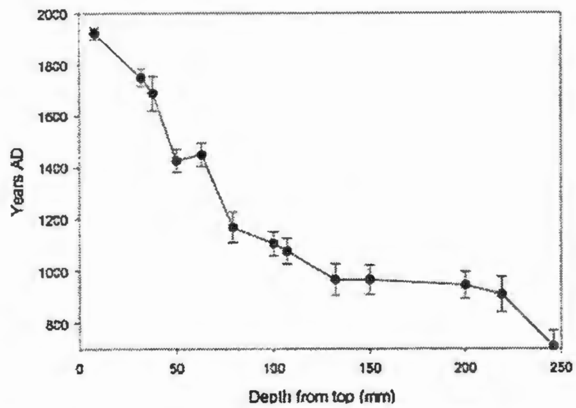

Figure 5. Tecoh Chronology based on thirteen dates.

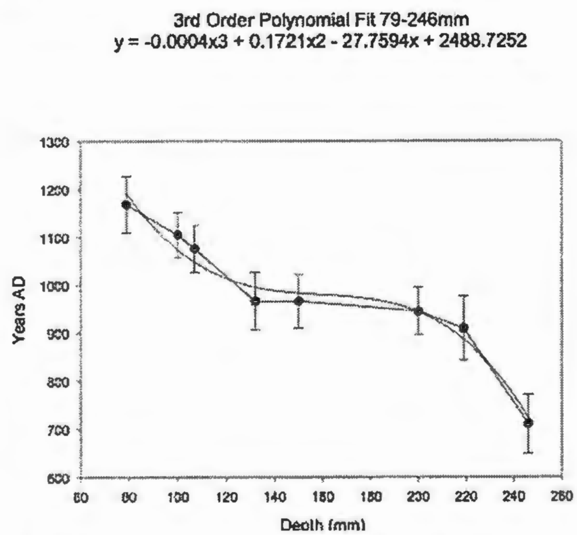

Figure 6. 3rd order polynomial fit used to develop age model for bottom 79-246 mm of Tecoh.

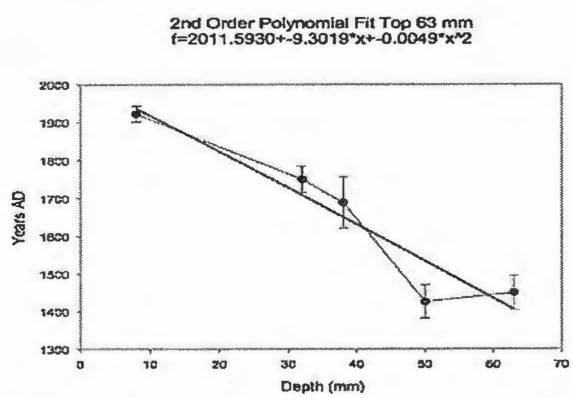

Figure 7. 2nd order polynomial fit used to develop age model for top 63 mm of Tecoh.

Table 2. Hobo 5 U/Th dates. Dates used to develop age model are boxed in. The error is 2σ error.

Sample Number	Depth (mm)	^{238}U (ppb)	^{232}Th (ppt)	$^{230}Th / ^{232}Th$ (atomic $x10^{-6}$)	$\delta^{234}U$* (measured)	$^{230}Th/^{238}U$	(activity)	^{230}Th Age (yr) (uncorrected)	^{230}Th Age (yr) (corrected)	$\delta^{234}U_{Initial}$** (corrected)	^{230}Th age (yr BP)*** (corrected)	^{230}Th age (yr AD/BC) (corrected)
H5-1	27	257.9 ±0.4	370 ± 13	63.7 ±10.2	-22.8 ± 2.0	0.00554	±0.00087	620 ± 97	**577 ± 99**	-22.8 ±2.0	**520 ± 99**	**1430 ± 99**
H5-32	32	250.0 ±0.5	163 ± 12	29.5 ±7.1	-24.4 ± 2.1	0.00117	±0.00027	130 ± 30	**111 ± 31**	-24.4 ±2.1	**54 ± 31**	**1896 ± 31**
H5-2	52	227.0 ±0.4	530 ± 15	41.9 ±1.7	-27.0 ± 1.6	0.00593	±0.00018	666 ± 21	**597 ± 41**	-27.0 ±1.6	**540 ± 41**	**1410 ± 41**
H5-3	72	184.3 ±0.3	273 ± 14	77.8 ±6.7	-25.0 ± 1.7	0.00701	±0.00049	786 ± 56	**742 ± 60**	-25.1 ±1.7	**685 ± 60**	**1265 ± 60**
H5-82	82	237.5 ±0.6	432 ± 13	76.5 ±7.9	-25.4 ± 2.5	0.00845	±0.00083	949 ± 94	**894 ± 98**	-25.4 ±2.5	**837 ± 98**	**1113 ± 98**
H5-110	110	208.2 ±0.4	1181 ± 12	24.4 ±1.6	-30.7 ± 1.9	0.00839	±0.00053	948 ± 60	**777 ± 104**	-30.8 ±1.9	**720 ± 104**	**1230 ± 104**
H5-4	116	210.9 ±0.4	2878 ± 32	15.6 ±0.4	-30.7 ± 2.1	0.01293	±0.00026	1,463 ± 30	**1052 ± 208**	-30.8 ±2.1	**995 ± 208**	**955 ± 208**
H5-126	126	97.2 ±0.1	1659 ± 12	12.1 ±1.2	-24.6 ± 2.6	0.01255	±0.00122	1,411 ± 138	**900 ± 290**	-24.7 ±2.6	**843 ± 290**	**1107 ± 290**
H5-135	135	179.1 ±0.4	2281 ± 15	13.4 ±1.2	-26.1 ± 2.8	0.01039	±0.00095	1,169 ± 108	**788 ± 219**	-26.1 ±2.8	**731 ± 219**	**1219 ± 219**
H5-141	141	194.2 ±0.5	#### ± 91	12.6 ±0.8	-25.8 ± 2.7	0.04902	±0.00290	5,626 ± 342	**3694 ± 1031**	-26.1 ±2.7	**3637 ± 1031**	**-1687 ± 1031**
H5-149	149	160.9 ±0.2	4805 ± 24	7.4 ±1.0	-28.1 ± 1.9	0.01348	±0.00189	1,522 ± 215	**624 ± 498**	-28.2 ±1.9	**567 ± 498**	**1383 ± 498**
H5-183	183	196.6 ±0.4	2417 ± 17	16.3 ±0.9	-27.9 ± 2.3	0.01220	±0.00067	1,376 ± 76	**1007 ± 199**	-27.9 ±15.2	**950 ± 199**	**1000 ± 199**
H5-5	207	236.7 ±0.4	670 ± 16	75.4 ±2.3	-30.2 ± 1.8	0.01294	±0.00025	1,464 ± 29	**1379 ± 51**	-30.3 ±1.8	**1322 ± 51**	**628 ± 51**
H5-215	215	176.6 ±0.4	187 ± 13	198.9 ±15.9	-25.8 ± 2.6	0.01275	±0.00054	1,436 ± 61	**1404 ± 63**	-25.9 ±2.6	**1347 ± 63**	**603 ± 63**

$\lambda_{230} = 9.1788 \times 10^{-6}\ y^{-1}$, $\lambda_{234} = 2.8263 \times 10^{-6}\ y^{-1}$, $\lambda_{238} = 1.55125 \times 10^{-10}\ y^{-1}$.

*$\delta^{234}U = ([^{234}U/^{238}U]_{activity} - 1)x1000$. ** $\delta^{234}U_{initial}$ was calculated based on ^{230}Th age (T), i.e., $\delta^{234}U_{initial} = \delta^{234}U_{measured} \times e^{\lambda_{234} \times T}$.

Corrected ^{230}Th ages assume the initial $^{230}Th/^{232}Th$ atomic ratio of $4.4 \pm 2.2 \times 10^{-6}$. Those are the values for a material at secular equilibrium, with the bulk earth $^{232}Th/^{238}U$ value of 3.8. The errors are arbitrarily assumed to be 50%.

***B.P. stands for "Before Present" where the "Present" is defined as the year 1950 A.D.

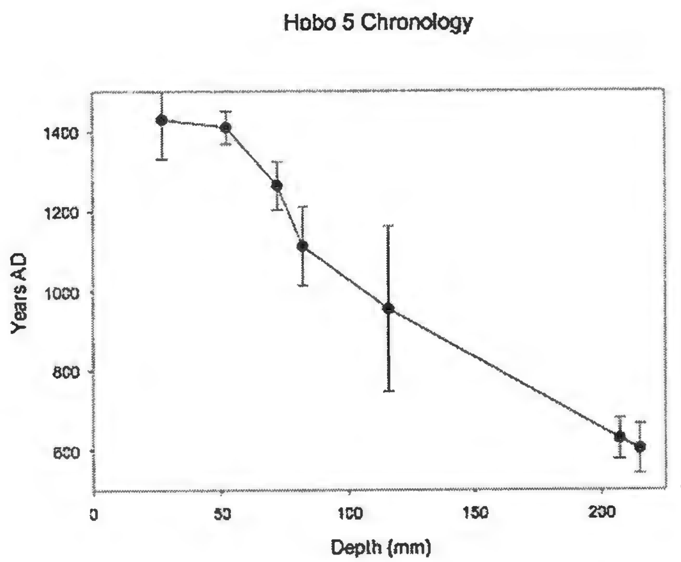

Figure 8. Hobo 5 chronology based on seven dates.

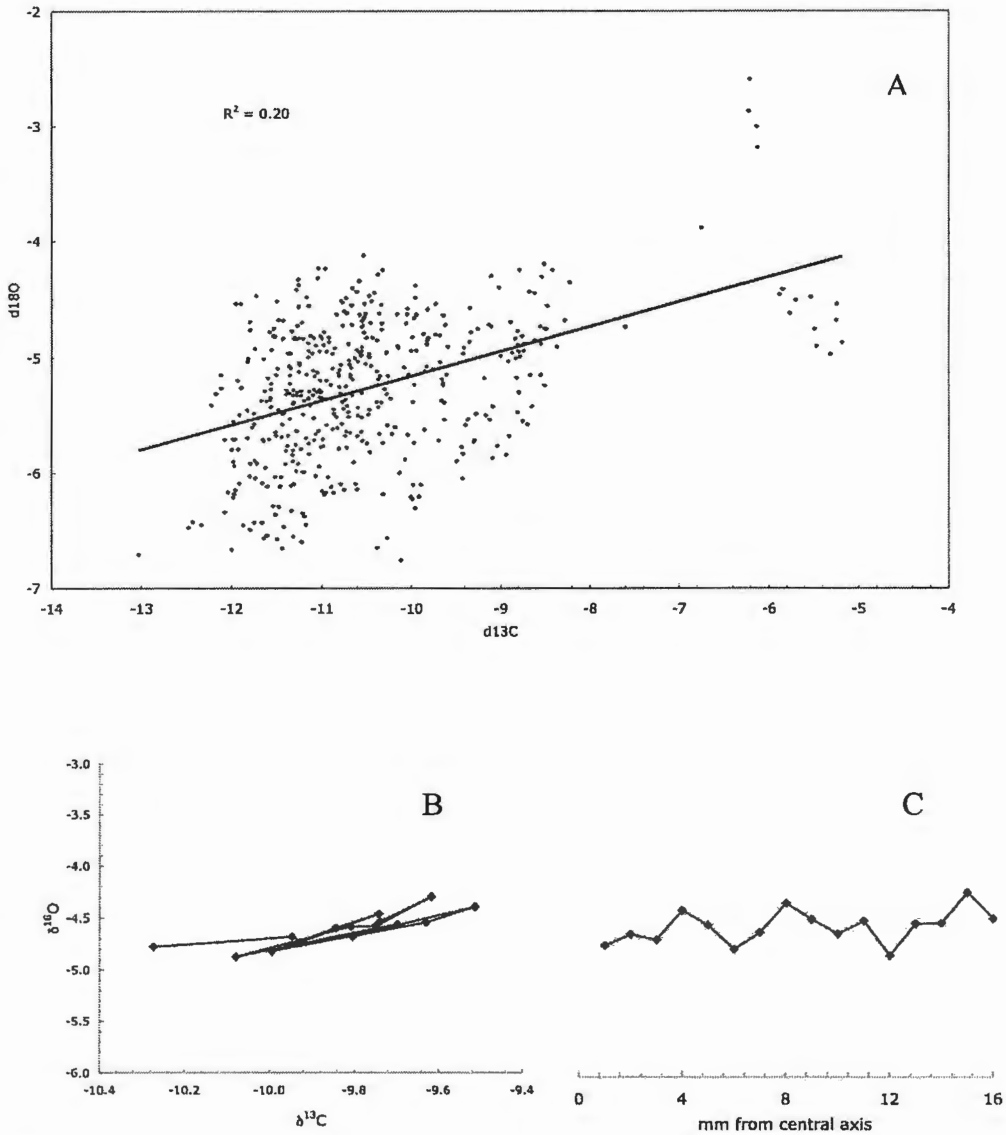

Figure 9. A. $\delta^{13}C$ vs. $\delta^{18}O$ from Tecoh stalagmite. Kinetic fractionation would produce a linear correlation. The low r^2 value (0.20) indicates a low degree of correlation, signifying the impact of kinetic fractionation is minimal. B. $\delta^{13}C$ vs. $\delta^{18}O$ from Hendy test at layer at 81 mm. C. $\delta^{18}O$ plotted versus distance from central axis, showing no significant variation in $\delta^{18}O$ with distance from the axis.

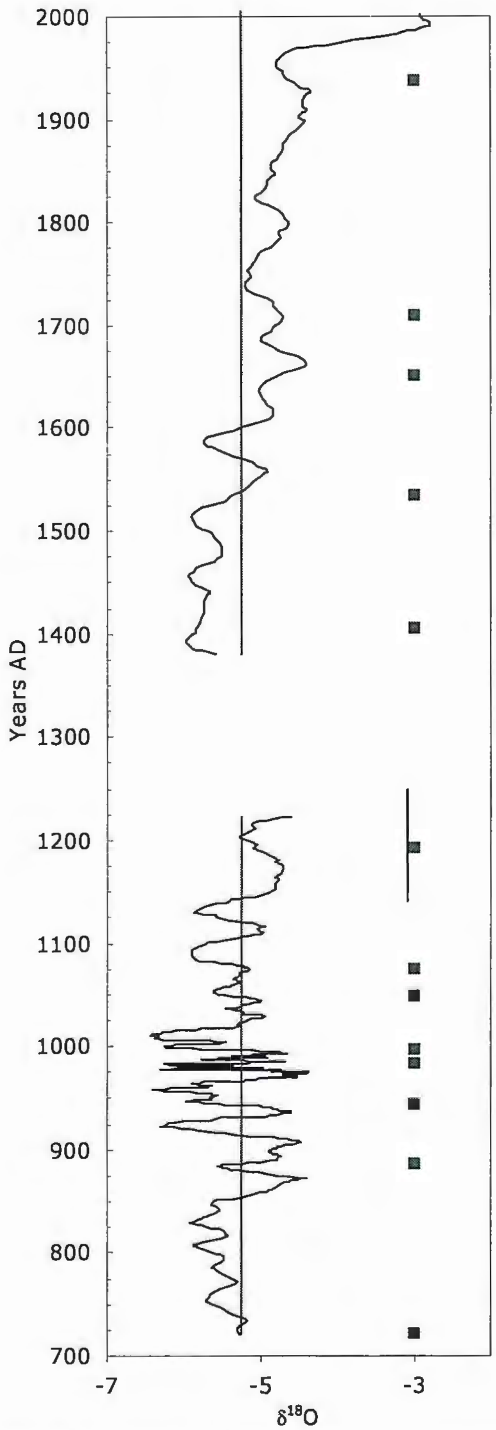

Figure 10. Tecoh δ18O profile. Mean δ18O speleothem value is shown as vertical line. Average error for each sample is shown by a vertical bar to the right of the curve.

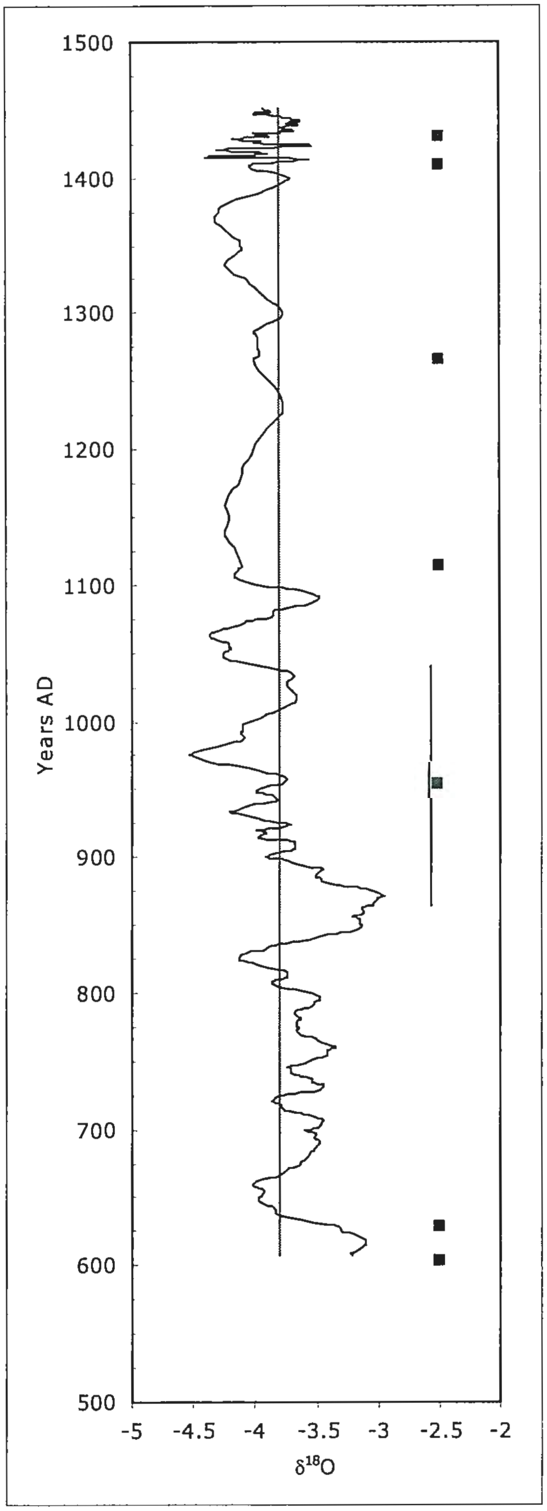

Figure 11. Hobo 5 δ18O profile. Mean δ18O speleothem value is shown as vertical line. Average error for each sample is shown by a vertical bar to the right of the curve.

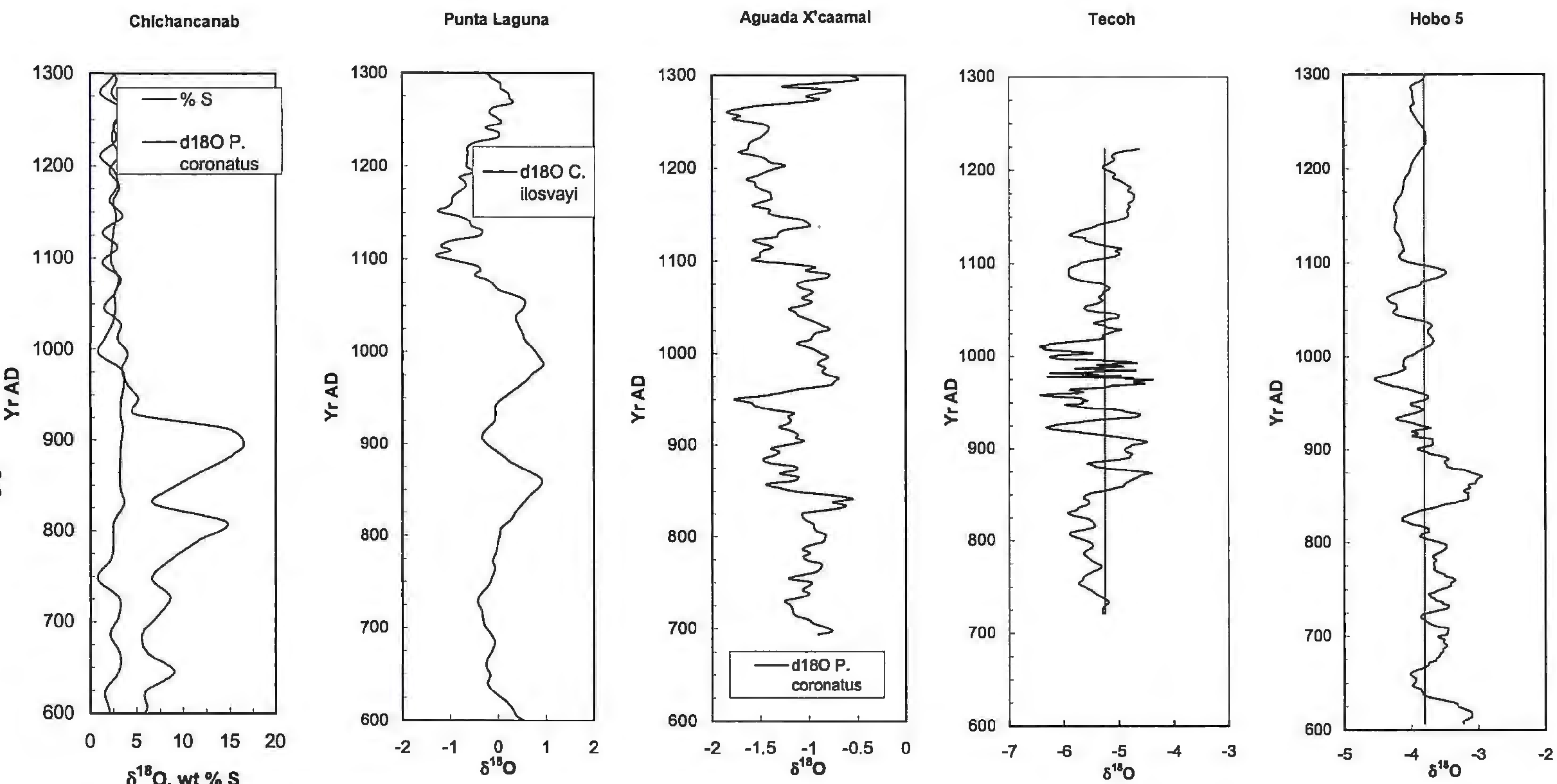

Figure 12. δ^{18}O data from 600-1300 AD for Yucatan lakes and speleothems.

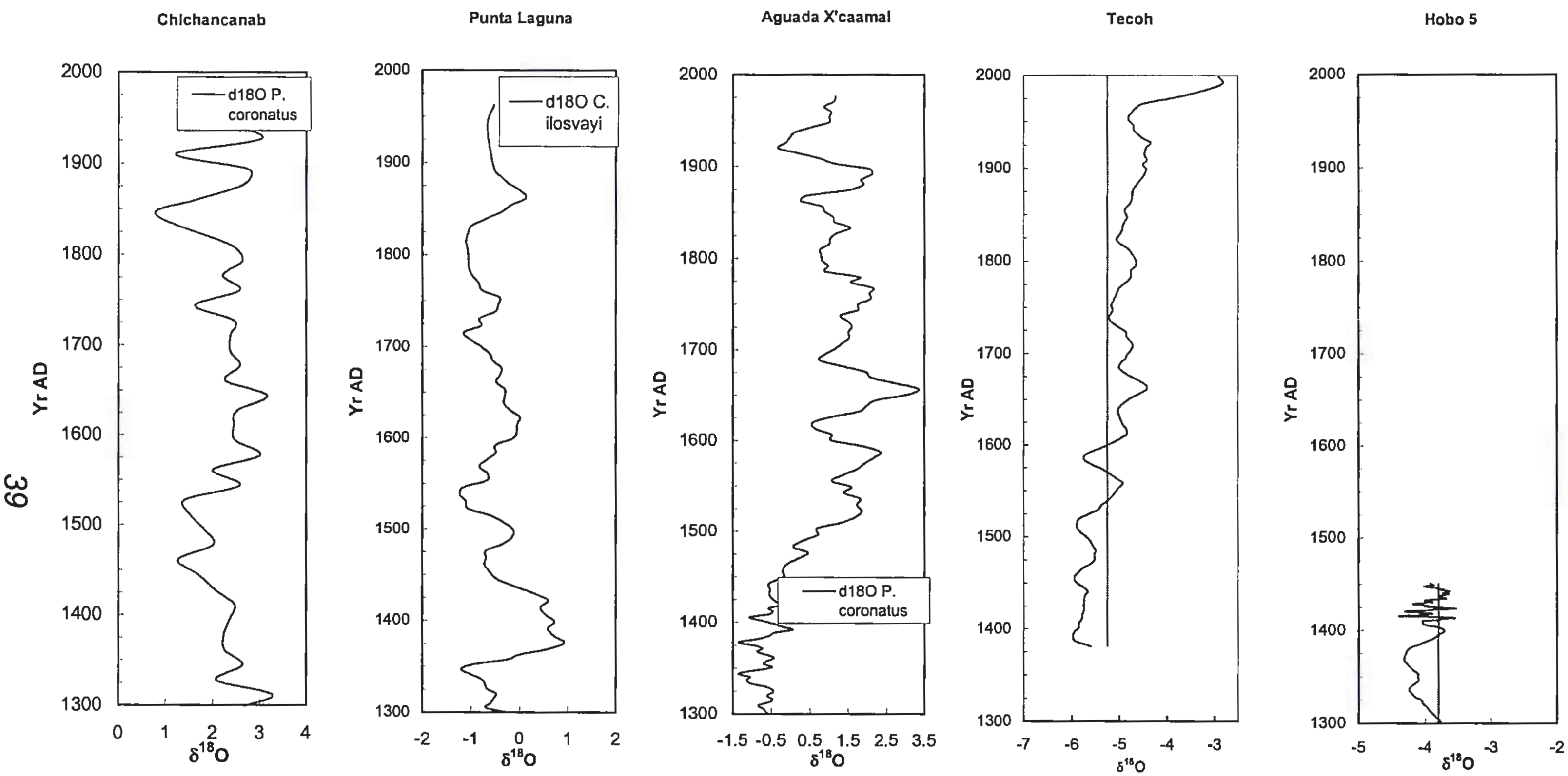

Figure 13. $\delta^{18}O$ data from 1300-2000 AD for Yucatan lakes and speleothems.

REFERENCES

Curtis, J.H., Brenner, M., Hodell, D.A., Balser, R.A., Islebe, G.A., Hooghiemstra, H., 1998. A multi-proxy study of Holocene environmental change in the Maya Lowlands of Peten, Guatemala. Journal of Paleolimnology 19, 139-159.

Curtis, J.H., Hodell, D.A., Brenner, M., 1996. Climate variability on the Yucatan Peninsula (Mexico) during the past 3500 years, and implications for Maya cultural evolution.Quaternary Research 46, 37-47.

Dorale, J.A., Edwards, R.L., Alexander, E.C., Shen C.-C., Richards, D.A., Cheng, H., 2004. Uranium-series dating of speleothems: current techniques, limits, and applications. In: Studies of Cave Sediments: Physical and Chemical Records of Paleoclimate, Sasowsky, I.D., Mylroie, J. (Eds.), Kluwer, New York, pp. 177-197.

Edwards, R.L., Chen, J.H., Wasserburg, G.J., 1987. ^{238}U-^{234}U-^{230}Th-^{232}Th systematics and the precise measurement of time over the past 500,000 years. Earth and Planetary Science Letters 81, 175-192.

Gill, R.B., 2000. The great Maya droughts: water, life and death. University of New Mexico Press, Albuquerque, pp. 326-333.

Harmon, R.S., Schwarcz, H.P., Gascoyne, M., Hess, J.W., Ford, D.C., 2004. Paleoclimate information from speleothems: the present as a guide to the past. In: Studies of Cave Sediments: Physical and Chemical Records of Paleoclimate, Sasowsky, I.D., Mylroie, J. (Eds.), Kluwer, New York, pp. 199-226.

Haviland, W., 1969. A new population estimate for Tikal, Guatemala. American Antiquity 34, 424-433.

Haug, G.H., Gunther, D., Peterson, L.C., Sigman, D.M., Hughen, K.A., Aeschlimann, B., 2003. Climate and the collapse of Maya civilization. Science 299, 1731-1735.

Hendy, C.H., 1971. The isotopic geochemistry of speleothems – I. The calculation of the effects of different modes of formation on the isotopic composition of speleothems and their applicability as paleoclimatic indicators. Geochimica et Cosmochimica Acta 35, 801-824.

Hodell, D.A., Brenner, M., Curtis, J.H., 2007. Climate and cultural history of the Northeastern Yucatan Peninsula, Quintana Roo, Mexico. Climatic Change 83, 215-240.

Hodell, D.A., Brenner, M., Curtis, J.H., Medina-Gonzalez, R., Ildefonso-Chan Can, E., Albornaz-Pat, A., Guilderson, T.P., 2005. Climate change on the Yucatan Peninsula during the Little Ice Age. Quaternary Research 63, 109-121.

Hodell, D.A., Brenner, M., Curtis, J.H., Guilderson, T., 2001. Solar forcing of drought frequency in the Maya lowlands. Science 292, 1367-1370.

Hodell, D.A., Curtis, J.H., Brenner, M., 1995. Possible role of climate in the collapse of Classic Maya civilization. Nature 375, 391-394.

Lachniet, M.S., Asmerom, Y., Burns, S.J., Patterson, W.P., Polyak, V.J. and Seltzer, G.O., 2004. Tropical Response to the 8200 yr BP cold event? Speleothem isotopes indicate a weakened early Holocene monsoon in Costa Rica. Geology, 32: 957-960.

Lachniet, M.S., Burns, S.J., Piperno, D.R., Asmerom, Y., Polyak, V.J., Moy, C.M. and Christenson, K., 2004. A 1500 year El Niño/Southern Oscillation and rainfall history for the Isthmus of Panama from speleothem calcite. Journal of Geophysical Research, D, Atmospheres, v. 109. DZ0117/1-8.

Leyden, B.W., 2002. Pollen evidence for climatic variability and cultural disturbance in the Maya lowlands. Ancient Mesoamerica 13, 85-101.

Leyden, B.W., Brenner, M., Hodell, D.A., Curtis, J.H., 1994. Orbital and internal forcing of climate on the Yucatan Peninsula for the past ca. 36 ka. Palaeogeography, Palaeoclimatology, Palaeoecology 109, 193-210.

Li, W.X., Lundberg, J., Dickin, A.P., Ford, D.C., Schwarcz, H.P., McNutt, R., Williams, D., 1989. High precision mass-spectrometic uranium series dating of cave deposits and implications for paleoclimate studies. Nature 339, 534.

Mestaz-Nuñez, A.M., Zhang, C., Albrecht, B.A., Enfield, D.B., 2002. Warm season water vapor fluyes in the Intra-Americas Sea. 27th Annual Climate Diagnostics and Prediction Workshop, Fairfax, VA, 21-25 October.

Morley, S.G., Brainerd, G.W., 1983. The Ancient Maya. Stanford University Press, Stanford, California, pp.1-43.

Perry, E., Velasquez-Oliman, G., Marin, L., 2002. The hydrogeochemistry of the karst aquifer system of the Northern Yucatan Peninsula, Mexico. International Geology Review 44, 191-221.

Rozanski, K., Araguá-Araguá, L., Gonfiantini, R., 1993. Isotopic patterns of modern global precipitation. In: Swart, P.K., Lohmann, K.C., McKenzie, J.A., and Savin, S. (Eds.), Climate Change in Continental Isotopic Records, American Geophysical Union, Washington, pp. 1-36.

Rosenmeier, M.F., Hodell, D.A., Brenner, M., Curtis, J.H., Martin, J.B., Anselmetti, F.S., Ariztegui, D., Guilderson, T.P., 2002. Influence of vegetation change on watershed hydrology: Implications for paleoclimatic interpretation of lacustrine 18O records. Journal of Paleolimnology 27, 117-131.

Sharer, R.J., 1994. The ancient Maya. Stanford University Press, Stanford, California. pp. 467-473.

Shen, C-C., Edwards, R.L., Cheng, H., Dorale, J.A., Thomas, R.B., Moran, S.B., Weinstein, S.E., Edmonds, H.N., 2002. Uranium and thorium isotopic and concetration measurements by magnetic sector inductively coupled plasma mass spectrometry. Chemical Geology 185, 165-178.

Turgeon, S.C., Lundborg, J., 2004. Establishing a speleothem chronology for Southwestern Oregon: climatic controls and growth modeling. In: Studies of Cave Sediments: Physical and Chemical Records of Paleoclimate, Sasowsky, I.D., Mylroie, J. (Eds.), Kluwer, New York, pp. 273-302.

Webster, J.W., Brook, G.A., Railsback, L.B., Cheng, H., Edwards, R.L., Alexander, C., Reeder, P.P., in press. Stalagmite evidence from Belize indicating significant droughts at the time of Preclassic abandonment, the Maya hiatus, and the Classic Maya collapse. Paleogeography.

Weidie, A.E., 1985. Geology of the Yucatan platform. In: Geology and hydrogeology of the Yucatan and Quaternary geology of the Northeastern Yucatan Peninsula, Ward, W.C., Weidie, A.E., Back, W., New Orleans Geological Society, New Orleans, Louisiana, pp.1-19.

White, W.B., 2004. Paleoclimate records from speleothems in limestone caves. In: Studies of Cave Sediments: Physical and Chemical Records of Paleoclimate, Sasowsky, I.D., Mylroie, J. (Eds.), Kluwer, New York, pp. 135-175.

Appendix A: U/Th Chemical Procedures

1. transfer powdered sample to a pre-weighed 30 ml Teflon vial and reweigh
2. cover sample with deionized water and then dissolve by adding small amounts of 7N HNO_3
3. spike dissolved sample using a solution with known concentrations of ^{233}U, ^{236}U, and ^{229}Th isotopes, and dry down on a hot plate
4. dissolve sample using 10-12 drops of $HClO_4$ to dissolve organics and to convert the sample to a uniform oxidation state, and then dry down again
5. while warm, dissolve again using 2N HCl, and then add a drop of Fe solution
6. coprecipitate U and Th with iron hydroxide by adding drops of concentrated NH_4OH
7. centrifuge solution and discard supernate
8. dissolve precipitate using 14N HNO_3 and dilute with 7N HNO_3 and dry down
9. dissolve sample using 2-3 drops of $HClO_4$ and dry down again
10. dissolve sample using 7N HNO_3, and transfer to an elution column containing anion exchange resin
11. elute thorium using 3 column volumes of 6N HCl; elute uranium using 4 column volumes of super clean H_2O; dry down U and Th separates
12. dissolve sample using 1-2 drops of $HClO_4$ and dry down again
13. dissolve separates in 14N HNO_3 and then dilute with a 1% HNO_3/HF solution
14. transfer to ICP vials in preparation for mass spectrometric analyses

Yucatan Samples

^{230}Th dating results. The error is 2σ error.

Sample Number	Depth (mm)	^{238}U (ppb)	^{232}Th (ppt)	^{230}Th / ^{232}Th (atomic x10^{-6})	δ^{234}U* (measured)	^{230}Th/^{238}U (activity)	^{230}Th Age (yr) (uncorrected)	^{230}Th Age (yr) (corrected)	$\delta^{234}U_{Initial}$** (corrected)	^{230}Th age (yr BP)*** (corrected)
OX-1-B	base	205.8 ±0.6	1006 ± 17	1071.4 ±25.3	271.7 ± 4.7	0.31786 ±0.00533	31,004 ± 611	**30895 ± 613**	296.5 ±5.2	**30838 ± 613**
OX-2-B	base	131.2 ±0.3	16258 ± 70	37.3 ±1.0	229.8 ± 4.6	0.28085 ±0.00779	28,012 ± 887	**25082 ± 1719**	246.7 ±5.0	**25025 ± 1719**
OX-3-T	top	158.1 ±0.5	3579 ± 22	31.9 ±1.3	406.1 ± 5.9	0.04386 ±0.00181	3,447 ± 145	**2979 ± 276**	409.5 ±6.0	**2922 ± 276**
OX-3-B	base	123.1 ±0.2	792 ± 15	139.7 ±6.1	412.5 ± 4.5	0.05458 ±0.00216	4,285 ± 173	**4153 ± 185**	417.4 ±4.5	**4096 ± 185**
IX-1x-B	base	193.6 ±0.4	5953 ± 27	119.1 ±2.3	568.7 ± 4.0	0.22227 ±0.00422	16,497 ± 338	**15935 ± 439**	594.9 ±4.3	**15878 ± 439**
IX-1-T	top	92.3 ±0.3	1095 ± 13	13.6 ±2.3	606.7 ± 7.9	0.00978 ±0.00162	665 ± 111	**450 ± 154**	607.5 ±8.0	**393 ± 154**
IX-1-B	base	130.3 ±0.2	2432 ± 14	78.2 ±2.1	503.2 ± 4.1	0.08853 ±0.00235	6,592 ± 181	**6232 ± 255**	512.1 ±4.2	**6175 ± 255**
IX-2-B	base	46.9 ±0.1	98 ± 13	7708.2 ±1049.1	12.9 ± 5.1	0.97500 ±0.01156	346,606 ± 38719	**346547 ± 38695**	34.2 ±25.5	**346490 ± 38695**
AC-B	base	59.1 ±0.1	4107 ± 17	108.3 ±1.8	232.7 ± 5.3	0.45664 ±0.00723	49,606 ± 1018	**48000 ± 1288**	266.5 ±6.1	**47943 ± 1288**
TE-3-B	base	572.9 ±1.7	2057 ± 15	250.3 ±4.0	27.4 ± 3.0	0.05457 ±0.00080	5,945 ± 92	**5843 ± 105**	27.9 ±15.5	**5786 ± 105**
CA-1-T	top	49.2 ±0.1	663 ± 12	7.6 ±1.7	151.5 ± 4.0	0.00622 ±0.00135	590 ± 128	**250 ± 213**	151.6 ±4.0	**193 ± 213**
PL-1-T	top	119.7 ±0.2	999 ± 12	26.3 ±1.5	224.8 ± 2.7	0.01330 ±0.00074	1,189 ± 67	**991 ± 119**	225.4 ±2.7	**934 ± 119**
PL-1-B	base	91.9 ±0.2	1040 ± 13	24.2 ±2.6	180.9 ± 4.3	0.01663 ±0.00177	1,544 ± 166	**1265 ± 216**	181.5 ±4.3	**1208 ± 216**
PL-2-T	top	83.0 ±0.1	2285 ± 13	14.6 ±1.4	136.1 ± 3.2	0.02439 ±0.00229	2,364 ± 224	**1657 ± 419**	136.7 ±3.2	**1600 ± 419**
PL-2-B	base	236.9 ±0.7	4038 ± 23	29.8 ±1.2	325.7 ± 4.6	0.03081 ±0.00127	2,559 ± 107	**2185 ± 216**	327.7 ±4.6	**2128 ± 216**
SR-T	top	175.0 ±0.3	769 ± 14	2104.2 ±42.3	74.5 ± 3.1	0.56159 ±0.00480	79,702 ± 1062	**79585 ± 1063**	93.2 ±3.9	**79528 ± 1063**
SR-B	base	177.4 ±0.3	167 ± 11	10079.7 ±665.9	82.4 ± 2.8	0.57544 ±0.00423	81,628 ± 952	**81603 ± 952**	103.7 ±53.7	**81546 ± 952**

$\lambda_{230} = 9.1788 \times 10^{-6}\ y^{-1}$, $\lambda_{234} = 2.8263 \times 10^{-6}\ y^{-1}$, $\lambda_{238} = 1.55125 \times 10^{-10}\ y^{-1}$.

*$\delta^{234}U = ([^{234}U/^{238}U]_{activity} - 1) \times 1000$. ** $\delta^{234}U_{initial}$ was calculated based on ^{230}Th age (T), i.e., $\delta^{234}U_{initial} = \delta^{234}U_{measured} \times e^{\lambda_{234} \times T}$.

Corrected ^{230}Th ages assume the initial $^{230}Th/^{232}Th$ atomic ratio of 4.4 ±2.2 x10^{-6}. Those are the values for a material at secular equilibrium, with the bulk earth $^{232}Th/^{238}U$ value of 3.8. The errors are arbitrarily assumed to be 50%.

***B.P. stands for "Before Present" where the "Present" is defined as the year 1950 A.D.

Appendix C: Map of Grutas Tzabnah

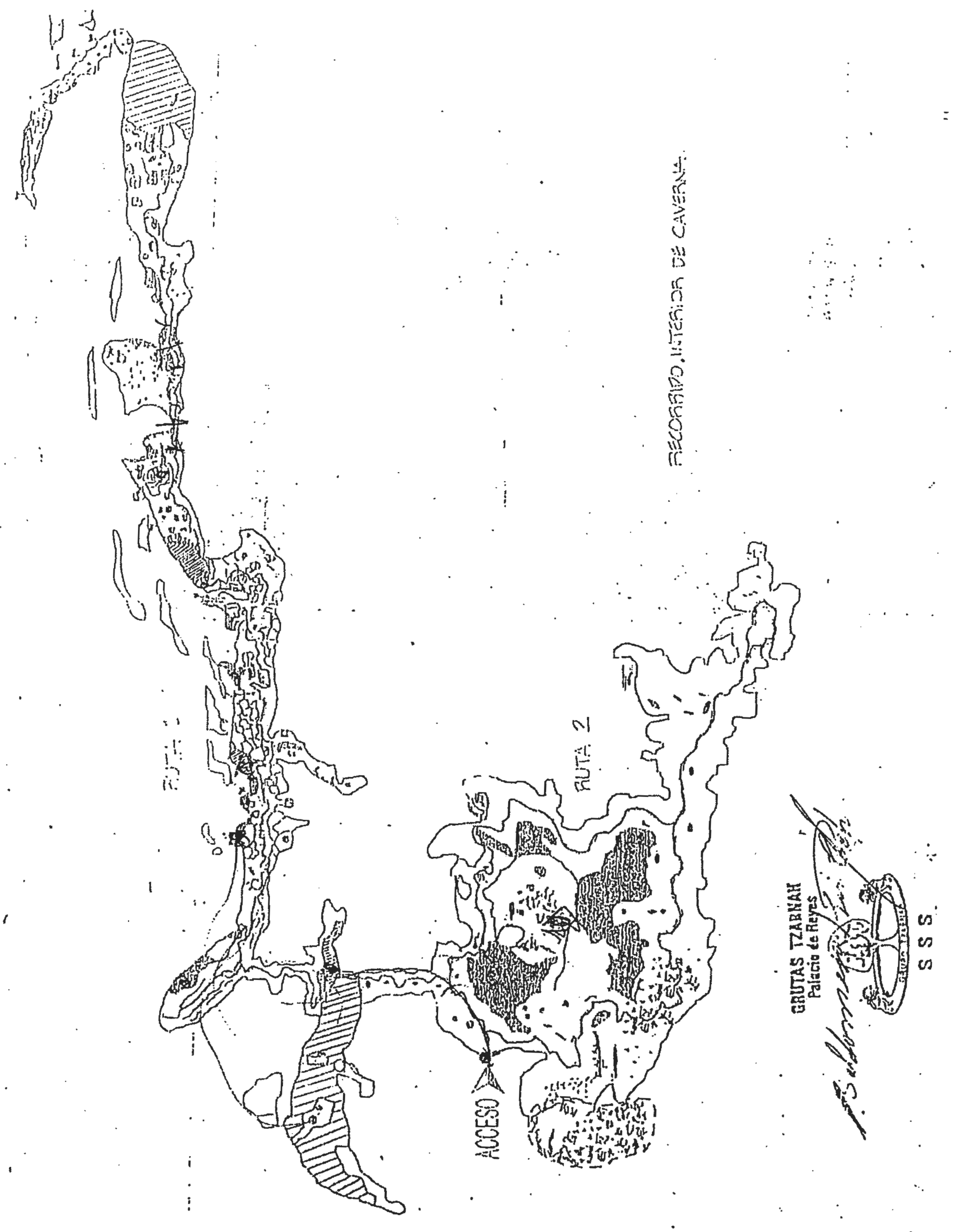

Appendix D: Map of Cueva Columnas

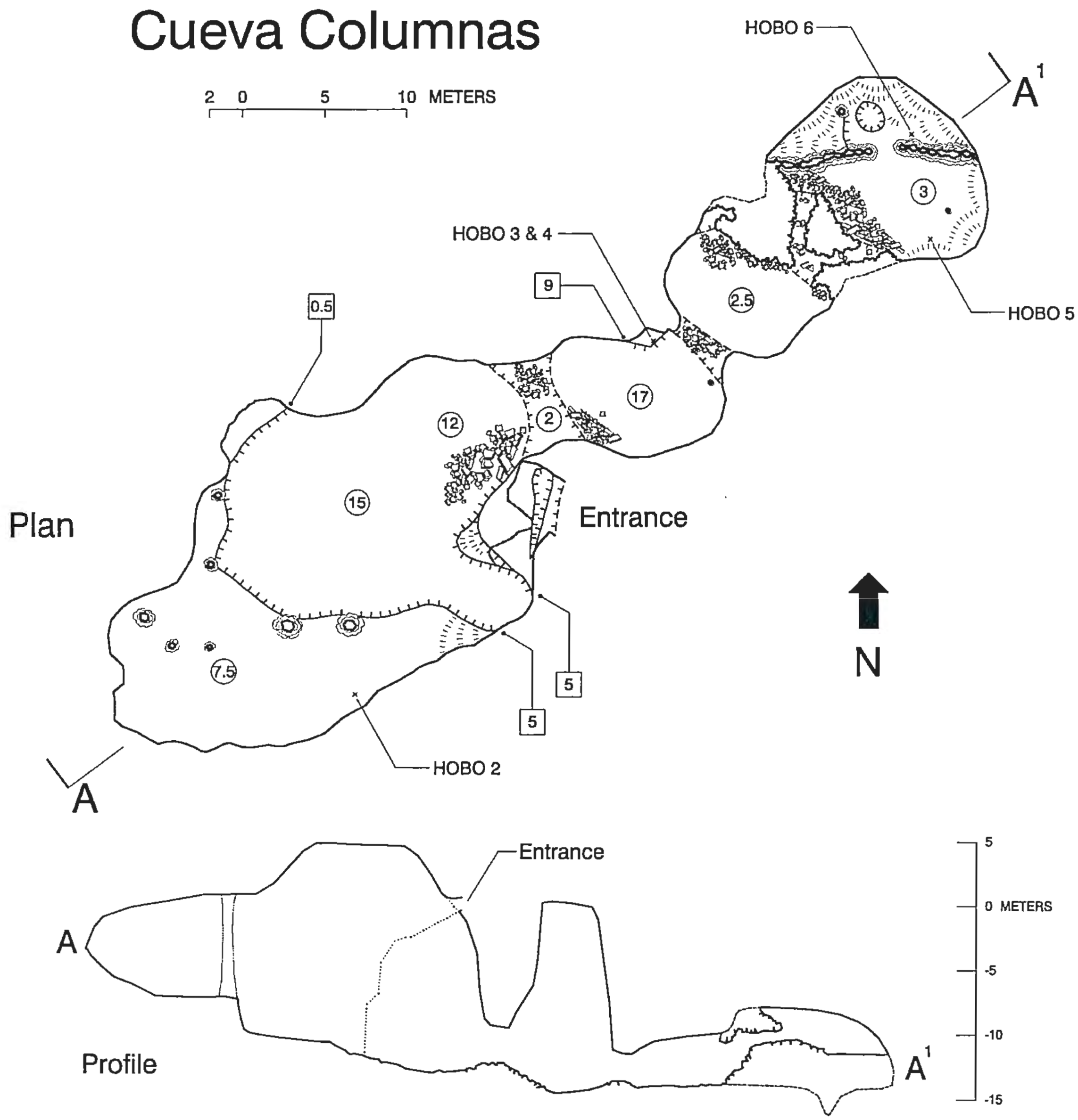

Map by Cara Gentry